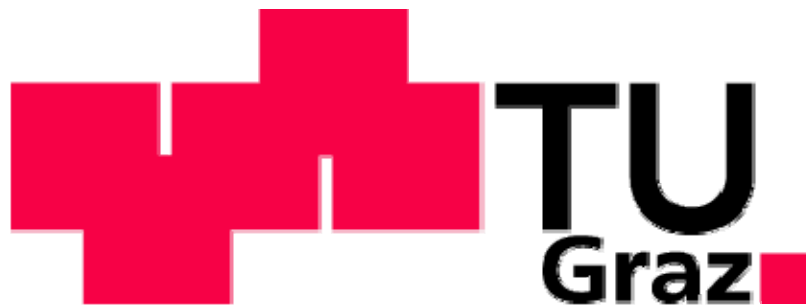


**Nnaemeka NDODO**

# **MPG-mediated delivery of small RNAs into human mesenchymal stem cells during proliferation and adipocyte differentiation**

Master Thesis



Institute for Genomics and Bioinformatics  
Graz University of Technology  
Petersgasse 14, 8010 Graz  
Head: Univ.-Prof. Dipl.-Ing. Dr.techn. Zlatko Trajanoski

Supervisor:  
Dr.rer.nat. Marcel Scheideler

Evaluator:  
Univ.-Prof. Dipl.-Ing. Dr.techn. Zlatko Trajanoski

Graz, December, 2007

## Table of content

1. INTRODUCTION .....	8
1.1. RNA Interference (RNAi) .....	8
1.2. Small non-coding RNAs .....	9
1.2.1. siRNA .....	9
1.2.2. MicroRNA .....	10
1.3. RNA delivery .....	12
1.3.1. Stable integration .....	12
1.3.2. Transient internalization .....	13
1.3.3. Lentiviral-mediated RNA delivery .....	13
1.3.4. Advantages .....	13
1.3.5. Disadvantages .....	13
1.3.6. CPP-mediated RNA delivery .....	14
1.3.7. Advantages .....	14
1.3.8. Disadvantages .....	15
1.4. Mechanism of Action .....	15
1.5. Types of cell-penetrating peptides .....	15
1.6. Examples of cell-penetrating peptides .....	16
1.6.1. MPG .....	16
1.6.2. Penetratin .....	18
1.6.3. Tat peptide .....	18
1.6.4. Transportan .....	19
1.6.5. Lologomers .....	19
1.7. Stem cells .....	19
1.7.1. Adult stem cells .....	20
1.7.2. Human multipotent adipose-derived stem (hMADS) cells .....	22
1.7.3. Adipocyte differentiation .....	22
1.7.4. MicroRNAs targeting adipogenesis .....	23
1.8. Objectives .....	24
2. MATERIAL AND METHODS .....	25
2.1. Material .....	25
2.1.1. Cell Culture of hMADS cells .....	25
2.1.2. Proliferation medium constituents .....	25
2.1.3. Differentiation medium constituents .....	25
2.1.4. Materials for transfection of hMADS cells .....	25

2.1.5.	Equipment .....	26
2.2.	Methods .....	26
2.2.1.	Proliferation and Differentiation of hMADS Cells .....	26
2.2.2.	Preparation of transfection complex and internalization .....	26
2.2.3.	Preparation of 0.5x MPG Buffer .....	27
2.2.4.	Transfection .....	27
2.2.5.	Slide Preparation for Fluorescence microscopy .....	27
2.2.6.	Fluorescent microscopes .....	28
2.2.7.	Zeiss Axioimager epifluorescence microscope .....	28
2.2.8.	Oil -Red-O Staining .....	29
3.	RESULTS .....	30
3.1.	hMADS cells adipocyte differentiation .....	30
3.2.	MPG-mediated siRNA delivery into hMADS cells .....	31
3.3.	Viability after MPG-mediated siRNA delivery .....	31
3.3.1.	Does the transfection of pre-confluent cells with SMC affect cell viability? .....	31
3.3.2.	Transfection of confluent and differentiating hMADS cells with siRNA-MPG complex (SMC) does not affect cell viability .....	31
3.3.3.	Transfection of pre-confluent cells .....	32
3.3.4.	Transfection of confluent cells (24h post-transfection) .....	36
3.3.5.	The siRNA-MPG complex was able to deliver siRNA into confluent hMADS cells (48h post-transfection analysis) .....	39
3.3.6.	Transfection of confluent cells (72h post-transfection analysis) .....	40
3.3.7.	Transfection of differentiating cells at Day 3 .....	42
3.3.8.	siRNA-MPG complex is able to deliver double-stranded siRNA into differentiating hMADS cells (48h post-transfection analysis) .....	44
3.3.9.	Transfection of differentiating cells at Day 10 .....	46
4.	DISCUSSION .....	48
4.1.	Viability .....	48
4.2.	Differentiation .....	48
4.3.	siRNA delivery in proliferation and in adipocyte differentiation .....	48
4.4.	Pattern of delivery .....	49
5.	CONCLUSION .....	50
5.1.	Outlook .....	50
6.	ABBREVIATION .....	51
7.	APPENDIX .....	52

---

7.1. PROTOCOL FOR N-TER–NANOPARTICLE MEDIATED DELIVERY OF siRNA INTO (hMADS).....	52
8. LIST OF FIGURES .....	55
9. LIST OF TABLES .....	55
10. REFERENCE.....	56

## ACKNOWLEDGEMENT

I am very grateful to God for the opportunity to enroll for this program. I am very thankful! My appreciation goes to Professor Zlatko Trajanoski for granting me the opportunity to come to study in the Institute for Genomics and Bioinformatics. For his kindness and his support, I am most grateful.

My profound gratitude goes to my meticulous supervisor Dr Marcel Scheideler. I can't thank him enough for all he taught me within this period to capture his word to bring me up to 'European thinking'. I am very honoured to have worked in his lab. His flare for excellence and attention to details commands my admiration. He is an excellent mentor and advisor.

I wish to appreciate Dr. Christian Paar for her excellent teaching skill that made me enjoy cell culture a lot! Didi Rieder made an invaluable contribution that cannot be easily forgotten in the cause of this work in the area of axioimaging. The long hours we had to work together were deeply appreciated. I am equally grateful to Dr Anne Krogsdam for kind assistance in many ways. Dr Andreas Prokesch was equally very help, Nicole Golob and Claudia Neuhold for helping me with plasmid and RNA isolation. I am equally grateful to Ms. Bettina Stockinger for her assistance in administrative matters. Thanks to Rene Snajder for his powerful IT support. And every member of the Institute for Genomics and Bioinformatics: Dr Juliane Strauss for the Barbecue and Biomaterial. Professor List for being a very good teacher! Who tickled my fancy for molecular electronics. I am equally grateful to Professor Schwab, Professor Hermetter, Dr Pichler and others.

Finally, I am grateful to the Afro-Asian Institute for their invaluable support and help in many ways. It was a nice experience coming to Graz.

## ABSTRACT

### Introduction

The cellular membrane constitutes an effective barrier that protects the complex, yet highly ordered, intracellular compartment of the cell. Passage of molecules across this barrier is highly regulated and highly restricted, with molecular size and amphiphilicity being the most significant criteria. Cell penetrating peptides (CPPs) are a class of small cationic peptides that are able to defy the rules of membrane passage and gain access to the intracellular environment. MPG is one member of this class of cell penetrating peptides capable of translocating the impervious hydrophilic cell membrane to deliver non-covalently attached cargo. In this study MPG was used to deliver FAM-labelled siRNA into hMADS cells.

### Method

Confluent and differentiated hMADS cells were transfected for 4h with 30nM siRNA-MPG-complex (SMC) and the controls were overlaid with free siRNA (SO) and cell only (CO) which contained MPG buffer for 4h and then analysed after 24h, 48h and 72h incubation post-transfection for internalization of the siRNA complex using Zeiss Axioimager for fluorescence detection and localisation. The pre-confluent cells were transfected with 15 nM of SMC for 4h and incubated for 24h and 48h post-transfection under standard cell culture conditions.

### Result

There was no noticeable adverse morphological variation between the siRNA-MPG complex transfected groups and the 'free siRNA' and the 'cell only' overlaid groups in the pre-confluent, confluent and differentiated stage following above mentioned transfection procedure. There was also no observed mortality associated with transfection. The differentiation of the cells into adipocyte phenotype was observed normally in all the groups following induction with adipocyte differentiation cocktail. Bright fluorescence speckles were exclusively detected in the MPG-mediated siRNA delivery of pre-confluent, confluent and differentiating hMADS cells in the cytoplasm as well as in the nucleus 24h and 48h post-transfection. The efficiency of delivery 24h after transfection in the confluent cells was about 90%, in cells differentiating 3 days toward adipocytes about 80%, and 50-60% of the cells showed internalised siRNA-MPG complex even 48h and 72h post-transfection.

### Discussion

MPG is non-viral and non electroporation-based transfection method that efficiently delivered double stranded siRNA into cytoplasm and nuclei of hMADS cells during proliferation and adipocyte differentiation. That MPG mediated nuclear localization of siRNA in this study supports the observation of Divita and co-workers (Crombez et al., 2007b; Simeoni et al., 2005). The pattern of fluorescence was punctuated in distribution, which was in line with the report of Veldhoen and colleagues (Veldhoen et al., 2006b). In variance with Zaragosi et al (2007) MPG as non-electroporation and n based transfection agent efficiently delivered siRNA into hMADS cells.

### Conclusion

In this study we could show that MPG efficiently delivered double-stranded siRNA into human mesenchymal stem cells in proliferating, confluent and differentiating stages. The cell viability was not adversely affected while differentiation of hMADS cells proceeded normally. These results demonstrated that MPG is a very effective and robust non-viral based transfection agent, easy to apply to non-dividing adherent cells during proliferation and differentiation, without necessity of detaching. The siRNA could be still detected up to 6 days after transfection. Thus MPG is a valuable tool for transient gene and microRNA silencing *in vitro*.

**Key words:** transfection, siRNA delivery, CPPs, MPG, hMADS cells.

## 1. INTRODUCTION

Human multipotent adipose-derived stem (hMADS) cells provide a good model for studying cell fate decisions like adipogenesis (Rodriguez et al., 2004c). hMADS cells are mesenchymal stem cell derived from the stroma-vascular fraction of human adipose tissue. hMADS cell have shown great promise as model for studying adipogenesis, osteogenesis and chondrogenesis (Rodriguez et al., 2004b; Zaragosi et al., 2007c) However, hMADS cells are very difficult to transfect using most traditional non-viral methods like lipid based agents (Zaragosi et al., 2007c). Hence, this study will investigate MPG for the internalization of FAM-labeled double-stranded siRNA into hMADS cells.

### 1.1. RNA Interference (RNAi)

RNA interference (RNAi) is a potent silencing mechanism that is induced by the cellular invasion of double -stranded RNA (dsRNA) molecules, which in turn trigger degradation of endogenous mRNAs showing sequence complementarity with the dsRNA (Arenz and Schepers, 2003). It was discovered by Fire and colleagues in 1998 (Fire et al., 1998). This milestone discovery earned Fire and Mello a Noble prize in 2006. The word RNAi came as a result of the discovery in *Caenorhabditis elegans* that the injection of dsRNAs interferes with the expression of specific genes that contain a highly homologous region to the delivered dsRNA (Agami, 2002a).

RNAi is a ubiquitous mechanism in eukaryotic cells to suppress the expression of genes involved in the important cell processes of differentiation and survival (Dykxhoorn et al., 2006). RNAi machinery modulates gene expression by post-transcriptional mechanisms (Birmingham et al., 2006).

The introduction of dsRNAs into eukaryotic cells can elicit at least four different types of responses that can selectively suppress gene expression: inhibition of protein translation, degradation of mRNAs, transcriptional inhibition and chromosomal rearrangements (Fire, 1999). The major players in the process of RNAi are the enzymes Dicer and Argonaute, and a small RNA species, small interfering RNA (siRNA). The siRNA is processed from a longer dsRNA substrate. One of the strands that is the leading strand is used to enter the RNA-induced silencing complex (RISC), a multi-protein complex containing Argonaute protein through which siRNA directs the silencing effect. Dykxhoorn et al,(2006) noted that small double-stranded RNAs processed from long double-stranded RNAs or from transcripts that form stem-loops, silence gene expression by several mechanisms – by targeting mRNA for degradation, by preventing mRNA translation or by establishing regions of silenced chromatin. Of these mechanisms mRNA degradation is said to be the most robust and the most exploited for therapeutic use (Dykxhoorn et al., 2006). mRNA degradation occurs when one strand (the antisense or guide strand) of the siRNA (about 22 nucleotides in length) directs RISC that contains the RNA endonuclease Ago2 to cleave its target mRNA bearing a complementary sequence (Elbashir et al., 2001; Tuschl et al., 1999). Figure 1 shows the various outcome of gene silencing by endogenous and exogenous hairpin-like transcripts (Agami, 2002b).

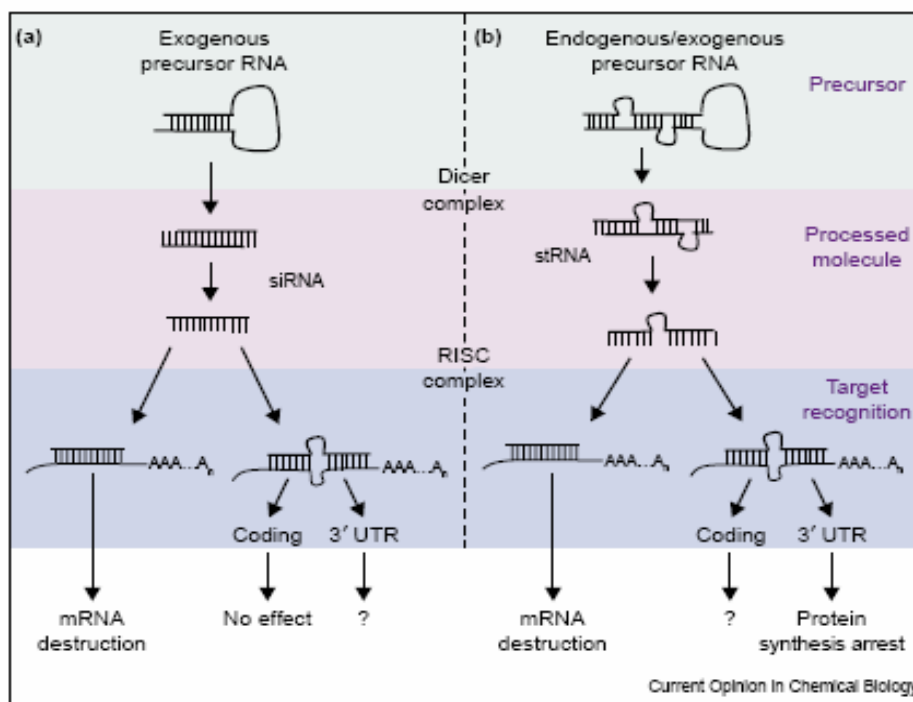


**Figure 1:** Gene silencing by endogenous and exogenous hairpin-like transcripts. A schematic model showing how **(a)** foreign siRNAs-like transcripts and **(b)** endogenous small temporal RNA (stRNAs) affect gene expression. Depending on the type of stRNA molecule and its target sequence, different outcomes are possible (Agami, 2002a)

## 1.2. Small non-coding RNAs

RNAs are split into two distinct classes: messenger RNAs (mRNAs), which are translated into proteins, and the non protein-coding RNAs (ncRNAs), which function at the RNA level. For many years it was believed that there were only a few ncRNAs, and they (e.g. tRNAs, rRNAs and spliceosomal RNAs) were considered accessory components to aid protein functioning (Huttenhofer et al., 2005).

### 1.2.1. siRNA

siRNA duplexes compose of 21-nt sense and 21-nt antisense strands, paired in a manner to have a 2-nt 3' overhang, are the most efficient triggers of sequence-specific mRNA degradation (Elbashir et al., 2002).

Small interfering RNAs were discovered by Hamilton and Baulcombe, as RNA species that are involved in post-transcriptional gene silencing (PTGS). Posttranscriptional gene silencing occurs in plants and fungi transformed with foreign or endogenous DNA and results in the reduced accumulation of RNA molecules with sequence similarity to the introduced nucleic acid. siRNAs contain a fully complementary dsRNA targeting sequence and require a perfectly matched target mRNA sequence for functionality (Agami, 2002a) directly into the target cell. Several studies have stipulated guidelines for the generation of siRNAs which are optimal in terms of efficacy and specificity. This includes the initial definition of the preferable length (19–25 bp) combined with a low G/C content in the range between 36% and 52% and the requirement of symmetric 2 nt overhangs at the 3'-end. siRNAs in which the helix at the 5' end of the antisense strand has a lower thermodynamic stability than the 3' end are generally more effective than those with the

opposite arrangement. A biochemical basis for the thermodynamic arrangement of effective siRNAs was provided by biochemical studies of the mRNA cleavage complex (RISC) in *Drosophila* embryo extracts, which demonstrated unequal incorporation of the two strands of the siRNA into RISC (Elbashir et al., 2002).

### 1.2.2. MicroRNA

MicroRNAs (miRNAs) are 21 to 24 nucleotide long RNA molecules that bind to partially complementary sequences within the 3'-untranslated region of target mRNAs leading to translation inhibition and/or degradation. miRNAs are encoded in the genome and are transcribed into primary miRNA (pri-miRNA) molecules. These pri-miRNAs are processed in the nucleus by the RNase III enzyme Drosha and its partner protein DGCR8 (Gregory et al., 2005). The resulting miRNA precursors (pre-miRNAs) are then transported to the cytoplasm by Exportin-5 (Lund et al., 2004). Finally, pre-miRNAs are further processed by the cytoplasmic RNase III enzyme Dicer, and the resulting mature miRNAs enter the RISC. The key components of the RISC complex are Argonaute (Ago) proteins which contain PAZ and PIWI domains. Four of these, Ago1 to Ago4, have been demonstrated to associate with miRNAs in humans (Liu et al., 2005).

miRNAs are a large FAMILY of regulatory RNAs expressed in metazoan animals and plants. They are processed from endogenous precursor molecules, which fold into dsRNA-like hairpins. With very few exceptions, animal miRNAs regulate gene expression by base pairing imperfectly to the 3'-untranslated region (3'-UTR) of target mRNAs, inhibiting protein synthesis by an unknown mechanism. By contrast, plant miRNAs generally show nearly precise complementarity to target mRNAs and trigger mRNA degradation via a mechanism similar to that operating during RNAi (Filipowicz et al., 2005).

miRNAs form part of RISC-like ribonucleoprotein particles, miRNPs or miRISCs, like siRNA. There is partial overlap in the protein composition of RISCs and miRNPs (for instance both complexes contain proteins of the Argonaute FAMILY), in line with the ability of miRNAs to act, in certain circumstances, as siRNAs and vice versa (Bartel, 2004).

MicroRNAs can also be said to be stem-loops that are processed into an imperfect complementary dsRNA that inhibit protein translation of an imperfectly matched target sequence which is located at the 3'UTR of the target mRNA (Agami, 2002a). miRNAs are thought to interact more frequently or more effectively with 3' UTRs than with other regions of mRNAs (Lim et al., 2005). Lim et al. showed that imperfect base-pairing leads to elaborate mRNA degradation of the target genes with far reaching implication for mRNA profiling in that field. Metazoan miRNAs have been implicated in directing cleavage reactions *in vivo*, for target sites with near-perfect complementarity (Yekta et al., 2004).

Tuschl group reported that *in vitro* experiments have shown that an RNA-inducing silencing complex (RISC) can cleave highly mismatched substrates (Martinez and Tuschl, 2004).

Lim and colleagues further speculated that subtle decreases in transcription levels could be independent of the RISC endonuclease, but might arise from the recruitment of other mRNA degradation machinery or as a secondary effect of inhibiting productive translation.

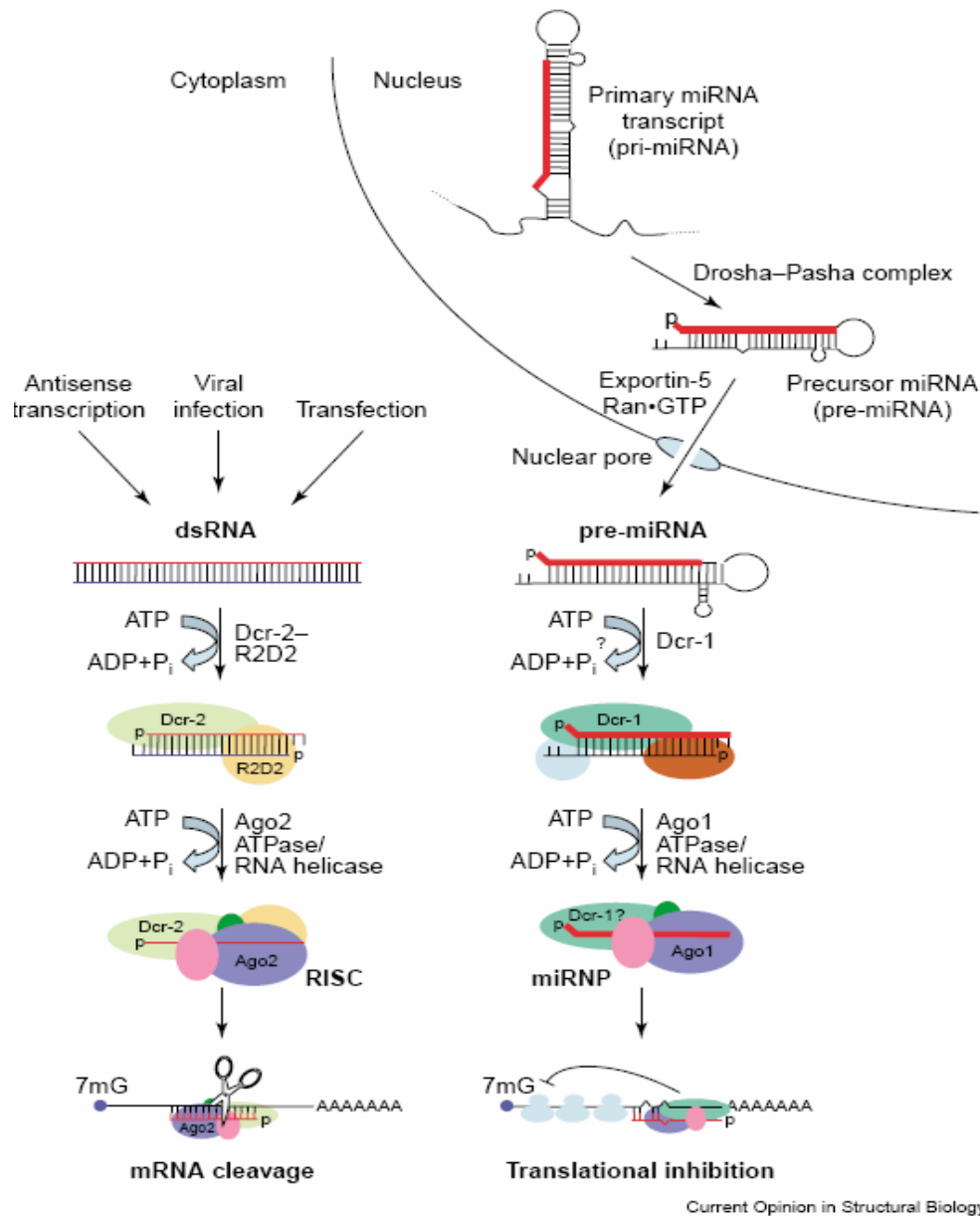


**Figure 2:** miRNA biogenesis and post-transcriptional gene regulation by miRNAs and siRNAs. The pathway shown is primarily based on data from *Drosophila*, although processing and assembly steps in mammalian cells are similar. Pri-miRNAs frequently contain more than one pre-miRNA hairpin. The Dcr-2–R2D2 complex recognizes the thermodynamic asymmetry of siRNA, with Dcr-2 binding to the less stable end of the duplex, near the 5' end of the selected guide strand. Rules of miRNA strand selection are similar, but details of the proteins involved are not known. Although not absolutely required, Dcr-1 also plays a role in siRNA-dependent RNAi. In mammals, a single Dicer participates in RNAi and miRNA pathways, but whether the protein is part of the mature RISC/miRNP is not yet established. *Drosophila* Ago1 and Ago2 function in miRNA and RNAi reactions, respectively. In mammals, all four Ago proteins, Ago1–4, seem to function in translational repression, but only Ago2 is a component of the cleavage-competent RISC. (Filipowicz et al., 2005)

### 1.3. RNA delivery

Delivery of biomolecules holds tremendous promise in the treatment of many genetic and acquired diseases. This became more imperative with the availability of human genome sequence data as well as other organismal platforms that are continually added into databases fuelling the demands for validation of target prediction.

However, identification of protein function and target validation require analytical tools to introduce or down-regulate genes. The main techniques used to “transiently silence” the expression of genes or proteins include the classical antisense oligonucleotides (ONs) and small interfering RNAs (siRNAs) as well as miRNAs. Another approach is introducing full-length proteins or genes of interest. Expressing those constructs would provide a direct way to analyze protein function. However, the inability of those hydrophilic molecules to enter cells is a major obstacle (El Andaloussi et al., 2005b).

Gary and colleagues suggested that the future of gene therapy in humans is dependent upon the discovery of safe and efficient vector system for transport of bio active molecules (Gary et al., 2007c).

A lot of efforts have been made to address the permeability of the membrane to hydrophilic molecules. Methods like electroporation, viral and other non-viral based delivery systems like lipofection, calcium sulphate, had been used to deliver different cargos across membrane with various degrees of success. Several delivery vectors, viral- and nonviral, have been developed to facilitate translocation of bioactive agents into cells. The viral vectors are by far the most effective delivery system but suffer from limited cargo carrying capacity, production problems, as well as possible viral recombination and immunogenicity *in vivo* (Gary et al., 2007b)

The efficient protection against enzymatic or non-enzymatic degradation is particularly important for RNA molecules including siRNAs. In fact, while the therapeutic potential of siRNAs for the treatment of various diseases is in principle very promising, limitations of transfer vectors may turn out to be rate-limiting in the development of RNAi-based therapeutic strategies (Aigner, 2006)

Aigner further suggested the use of DNA expression plasmids which encode palindromic hairpin loops with the desired sequence that upon transcription and folding of the RNA, the double-stranded short hairpin RNAs (shRNAs) are recognized by Dicer and cleaved into the desired siRNAs. This according to him would improve siRNA targeting (Aigner, 2006).

Attempts to improve RNA delivery have led to development of a number of delivery systems to circumvent observed limitations of current delivery tools.

Peptides represent a class of vectors that can be extensively modified to meet the needs of a particular gene delivery system. Critical to successful delivery of biomolecules like RNA is the ability to traverse the cell membrane and to release the cargo molecule safe from degradation while maintaining the integrity of the cell.

#### 1.3.1. Stable integration

Stable transfection is the type of transfection where genetic material that is introduced into a cell is retained beyond reproduction. In some transfections, DNA enters the cell nucleus and is integrated to or completely replaces the DNA of the eukaryotic cell. These are stable transfections. Only stable transfections allow the new DNA to be reproduced when the cell divides to create daughter cells. Under normal circumstances, it is difficult to produce a completely stable transfection; the tiny percentage of clones produced will soon die off and be replaced by cells with the original genetic material. Stable transfections that are experimentally useful are induced by co-transfecting another gene that can give the cell a selection advantage, typically resistance to a particular toxin. After mitosis, the cells

produced are exposed to the toxin. The cells with the co-transfection and the transfection desired will survive, while most of the normal cells will die. After many rounds of mitosis and toxin, only cells with the resistance and the desired genetic change will survive. Stable transfections are at the core of gene therapy. Only through a stable transfection can a faulty gene be permanently replaced.

### 1.3.2. Transient internalization

During transfection, foreign DNA, RNA, or peptides are introduced into eukaryotic cells. Experimentally, this is most often done as an instance of transient transfection, in which the transfected molecule is only transiently, that is, in only the cell to which it was originally integrated and only for a short period of time. This process is usually used to test how various genetic modifications affect the functioning of particular genes.

### 1.3.3. Lentiviral-mediated RNA delivery

Lentiviruses are a subclass of retroviruses that came to limelight in gene delivery due to their ability to stably transduce both dividing and non-dividing cells. Lentiviral vectors have been used to delivery RNA by many investigators in different cell types. Morris and colleague, reported that targeted suppression of HIV-1 had been achieved via siRNA targeting HIV-1 tat and rev transcript (Morris and Rossi, 2006b). Recently, Ren et al. (2007) described a novel approach based on lentiviral RNAi- mediated down-regulation of adenosine kinase (ADK), the major adenosine-removing enzyme, in human mesenchymal stem cells (hMSCs), which would be compatible with autologous cell grafting in patients. Following lentiviral transduction of hMSCs with anti-ADK miRNA expression cassettes they demonstrated up to 80% knock-down of ADK (Ren et al., 2007).

### 1.3.4. Advantages

Lentiviral vectors have inherent ability to stably transduce both dividing and non-dividing cells (Morris and Rossi, 2006a). Gene delivery is stable because the target gene or gene silencing sequence is integrated in the chromosome and is copied along with the DNA of the cell every time the cell divides. One of the defining features of Lentiviral system is their ability to integrate into non-dividing cells, in contrast to other vectors that either do not integrate efficiently into chromosomal DNA (e.g., non-viral, adenoviral and adenoviral-associated vectors), or can only integrate upon cell division (e.g., conventional retroviral vectors). Viral vectors have been used extensively in the delivery of nucleic acids. They have the advantage of high transfection efficacy due to the above mentioned features (Aigner, 2006).

### 1.3.5. Disadvantages

Viral systems show a limited loading capacity regarding that the genetic material are rather difficult to produce in a larger scale and, most importantly, pose severe safety risks due to their oncogenic potential and their inflammatory and immunogenic effects which prevent them from repeated administration. Lentiviral vectors suffer from limited cargo carrying capacity, production problems, as well as possible viral recombination (recombinant competent retrovirus) and immunogenicity *in vivo* (Gary et al., 2007a). Viruses tend not to disperse well in target tissue and often do not express their gene for long periods. Furthermore, in some acute disorders, viral vectors might not express sufficient amounts of the recombinant protein within a short period to be protective because of a compromised host cell metabolism

### 1.3.6. CPP-mediated RNA delivery

Many CPPs were designed from sequences of membrane interacting proteins, such as fusion proteins, signal peptides, transmembrane domains and antimicrobial peptides. Within these sequences, short sequences called protein transduction domains or PTDs proved to efficiently cross biological membranes without the need of a carrier or of a receptor and to deliver peptides. The major obstacle for using small RNAs as drugs is to deliver them into the cytoplasm of cells. An exception may be mucosal tissues. In the lung and vagina, siRNA uptake is extremely efficient and occurs even in the absence of transfection reagents (Dykxhoorn et al., 2006).

Improving internalization of siRNAs is a criterion in order to induce biological effects. According to (El Andaloussi et al., 2005a) there exist few instances of CPP-mediated delivery of antisense and siRNA. However both Tat and TP have been covalently linked to, and successfully used to deliver siRNAs against GFP and luciferase and a subsequent down regulation of proteins was observed (Muratovska and Eccles, 2004). MPG, was non-covalently complexed with siRNA directed against glyceraldehyde-3-phosphate dehydrogenase (GADPH) and significantly increased the uptake and silencing activity of siRNA (Simeoni et al., 2003)

Veldhoen and colleagues exploited the flexibility of a non-covalent strategy; by focusing on the characterisation of a novel carrier peptide termed MPG $\alpha$ , which spontaneously forms complexes with nucleic acids. (Veldhoen et al., 2006b) used a luciferase-targeted siRNA cargo; to address the cellular uptake mechanism of MPG $\alpha$ /siRNA complexes in HeLa cells. They showed a significant reduction of the RNA interference with MPG $\alpha$ /siRNA complexes in the presence of several inhibitors of endocytosis. Using confocal laser microscopy they observed a punctual intracellular pattern rather than a diffuse distribution of fluorescently labelled RNA-cargo. Their data suggested strong evidence of an endocytotic pathway contributing significantly to the uptake of MPG $\alpha$ /siRNA complexes (Veldhoen et al., 2006b)

### 1.3.7. Advantages

CPPs have been shown to efficiently improve intracellular delivery of various biologically active molecules into cells both *in vivo* and *in vitro* (Deshayes et al., 2005; El Andaloussi et al., 2005c). They are able to overcome both extracellular and intracellular limitations. These limitations include the impervious hydrophilic cell membrane as well as the intracellular endosomes that degrade delivered cargo. They can trigger the movement of a cargo across the cell membrane into the cytoplasm of the cells and improve its intracellular targeting, thereby facilitate the interaction with the target. The different cellular compartments (including the nucleus) are protected by biological membranes. These membranes segregate the various cellular compartments and prevent influx and efflux of solutes from cells and organelles. Although these barriers are essential for the maintenance of the cell, they can become a problem in cellular studies and must be overcome before the diverse processes occurring within the cell can be investigated (Jarver and Langel, 2004).

Most of the CPPs are covalently attached to their cargo by either chemical cross-linking or cloning (Crombez et al., 2007a). CPPs are able to transport various cargo types addressing various sub-cellular domains due to the various possible modifications arising from the peptide sequence. According to Deshayes and colleagues, some peptides used for delivery of nucleic acids, promote their delivery through the endosomal pathway, whilst others can cross membranes independent of the endosomal pathway like MPG and hence avoid degradation of the nucleic acid by endosomes. In spite of concerns about delivery pathways, *In vivo*, CPPs can cross the blood–brain barrier and mediate delivery to several organs (Dietz and Bahr, 2004). Targeted delivery by CPP is a possible goal, and recent reports show great promise in this field. Vector stability can be improved by using the D-form of the amino acid during design. The D-form is not degraded by proteases to the

same extent (as the L-form) and remains intact for a longer time when injected *in vivo*. Other possibilities are to use peptide mimics such as beta-peptides, or peptoids (Pooga et al., 1998).

There is an increasing need for an efficient, non-toxic, non-hazardous transport vector. Cell-penetrating peptides fulfill all of these criteria and may in the future be an important tool in pharmaceutical research.

Cell penetrating Peptide mediated delivery of biomolecules appears to be a technology that in many aspects is superior to commonly used delivery agents.

### 1.3.8. Disadvantages

Despite promising data from CPP studies, a clear description of their properties remains elusive. The CPP field has been under constant change during the years and the uptake mechanism still remains ambiguous. Several attempts have been made in order to elucidate the true mechanism of peptide mediated uptake, but the results are divergent between different reports and experiments. Even when using the same peptide, results vary between different groups (Jarver and Langel, 2006).

The main problem with using CPPs as gene delivery vectors is the lack of cell specific targeting. CPPs seem to penetrate virtually any cell type both *in vivo* and *in vitro*. That the peptides seem to enter any and every cell they get in contact with, might restrict CPP application as a pharmaceutical tool greatly. The delivery also seems to utilize a pathway(s) present in all cells. This common feature makes CPP applications complicated in pharmaceutical use. The stability of peptide vectors is another problem regarding *in vivo* delivery. If the vector does not remain intact until it reaches its target, it could do more harm than good. However, this problem could be circumvented by mostly using D-form instead of L-amino acid.

### 1.4. Mechanism of Action

Early investigation of mechanism of action of CPPs supported non-endosomal pathway however recently studies led to the complete revision of the cellular uptake mechanism of CPPs, incorporating the involvement of the endosomal pathway (Richard et al., 2003). However, as for most CPPs, evidence for several cell-entry routes have been reported, some of which are independent of the endosomal pathway (Deshayes et al., 2005), so it is essential to identify the one leading to a biological response.

Simeoni and colleagues showed that the presence of endosomal inhibitors like bafilomycin A and cytochalasin B did not alter gene expression, suggesting that the cellular uptake mechanism of MPG/DNA complexes is essentially independent of the endosomal pathway (Simeoni et al., 2003).

### 1.5. Types of cell-penetrating peptides

Cell-penetrating peptides (CPPs), equally referred to as protein transduction domains (PTDs), Trojan peptides or membrane translocating sequences (MTS), have shown significant potential in the field of drug delivery. CPPs can deliver a wide range of bioactive molecules such as proteins, peptides, oligonucleotides (ON), and nano-particles to several cell types and to different cellular compartments, both *in vivo* and *in vitro*. These peptides vary in size, amino acid sequence, and charge, but share the common feature that they have the ability to rapidly translocate the plasma membrane and enable delivery to the cytoplasm or nucleus (Lindgren et al., 2000).

According to Deshayes et al. (2005) CPPs are classified as follows with reference to peptides derived from protein transduction domains or their family for classification

reasons they include: (transportan, penetratin, Tat and VP22, amphipathic peptides (MAP KALA, ppTG20, proline-rich peptides), MPG-derived peptides (MPG and Pep-1) and three peptides which cannot be fit into the classes cited above (oligomers, arginine-rich peptides and calcitonin-derived peptides (Lindgren et al., 2000).

## 1.6. Examples of cell-penetrating peptides

### 1.6.1. MPG

MPG is a bipartite amphipathic peptide derived from both the fusion peptide domain of HIV-1 gp41 protein and the NLS of SV40 large T antigen. It forms stable non-covalent complexes with nucleic acids and promotes their delivery into a large number of cell lines (Simeoni et al., 2003). The positively charged NLS most likely interacts electrostatically with DNA and condenses the cargo while the hydrophobic gp41 domain mediates membrane fusion. Inside the cell, the NLS confers nuclear localization of cargo.

However, this localization can be affected by slight modifications in the NLS sequence, such as a K to S substitution, that lead to partial cytoplasmic release of the cargo, while no detectable effect can be observed on the free forms of the peptide (Deshayes et al., 2004; Simeoni et al., 2005; Simeoni et al., 2003). MPG successfully transfected a number of cell types, which include: 3T3-L1, differentiated adipocyte mouse embryonic fibroblast cell line, A2780 human ovarian carcinoma cell line, A549 human lung carcinoma cell line, ASPC-1 human pancreatic carcinoma cell line, Astrocyte human neuronal primary cell, Astrocytoma human neuronal astrocytoma cell line, BSMC, human bronchial smooth muscle primary cell, C2C12, differentiated myocyte mouse myoblastoma line, HeLa, human cervical adenocarcinoma cell line, HepG2, human hepatocarcinoma cell line, HT-29, human colorectal adenocarcinoma cell line, HUVEC, human umbilical vein epithelial primary cell, MCF7, human breast adenocarcinoma cell line, MDA-MB-231, human breast adenocarcinoma cell line, NHEK-AD, human adult keratinocyte primary cell, Raw264.7, mouse macrophage cell line, SW620, human colorectal adenocarcinoma cell line (<http://www.sigmaaldrich.com/sigma/bulletin/N0788bul.pdf>). MPG is important in targeting genes to the nucleus making this peptide an interesting vector for clinical trials.

### Structure of MPG

MPG is a 27-residue-long primary amphipathic peptide with the following sequences: (acetyl GALFLGFLGAAGSTMGAWSQPKKKRKVCysteamide) (Crombez et al., 2007b). The peptide contains three distinct domains: a N-terminal hydrophobic motif (GALFLGFLGAAGSTMGA) derived from the fusion sequence of the HIV-1 gp41 (glycoprotein 41), required for interaction with the lipid moiety of the cell membrane and cellular uptake, a hydrophilic domain derived from the NLS (nuclear localization sequence) of SV40 (simian virus 40) large T-antigen (KKKRKV) involved in the interactions with nucleic acids and intracellular trafficking of the cargo, and a linker domain (WSQP), which improves the flexibility and integrity of the hydrophobic and the hydrophilic domains (Crombez et al., 2007b). MPG carries a cysteamide group at its C terminus, which is essential for both cell entry and stabilization of the complexes with siRNA (Simeoni et al., 2003). MPG, originally designed to improve the cellular uptake of oligonucleotide and plasmid, was then optimized for the delivery of siRNA. A single mutation on the second lysine residue of the NLS to serine (MPG<sup>Δ</sup>NLS- GALFLGFLGAAGSTMGAWSQPKSKRKV), was shown to abolish the nuclear translocation and facilitate a rapid release of the siRNA in the cytoplasm (Simeoni et al., 2003).

### MPG Interaction with siRNA cargo

The MPG peptide associates rapidly in solution with siRNA, initial contact occurs through electrostatic interactions involving the hydrophilic lysine-rich domain independently of specific sequences, followed by peptide–peptide interactions involving the gp41 hydrophobic domain, thus generating stable MPG–siRNA nanoparticles with size of approx. 200 nm diameter (Simeoni et al., 2003). Studies by Simeoni and colleagues suggest MPG exhibits high affinity in the nanomolar range for siRNA and that approx. 10–20 peptide molecules are required to form a highly stable nanoparticle (Simeoni et al., 2003). The presence of a peptide-based nanostructure associated to the siRNA dramatically improved its stability inside the cell and significantly protected it from degradation (Crombez et al., 2007b).

### Mechanism of action of MPG

The internalization process of MPG according to Deshayes *et al.* (2004) is achieved through formation of a carrier/cargo complex and occurs through a non-endosomal pathway leading to a mainly nuclear final localization of the cargo. Simeoni and colleagues showed that the presence of endosomal inhibitors like bafilomycin A and cytochalasin B did not alter gene expression, suggesting that the cellular uptake mechanism of MPG/DNA complexes is essentially independent of the endosomal pathway (Simeoni et al., 2003). From structural point of view, Divita's group showed in greater details that the outer part of the 'carrier-based nanoparticle' with the siRNA plays a key role in the interactions of MPG with the membrane. MPG strongly interacts with phospholipids, through their hydrophobic fusion sequence, which then adopted a  $\beta$ -structure required for insertion of the peptide into the membrane (Deshayes et al., 2004). On the basis of both structural and biological investigations, they proposed a four-step mechanism as illustrated in Figure 3:

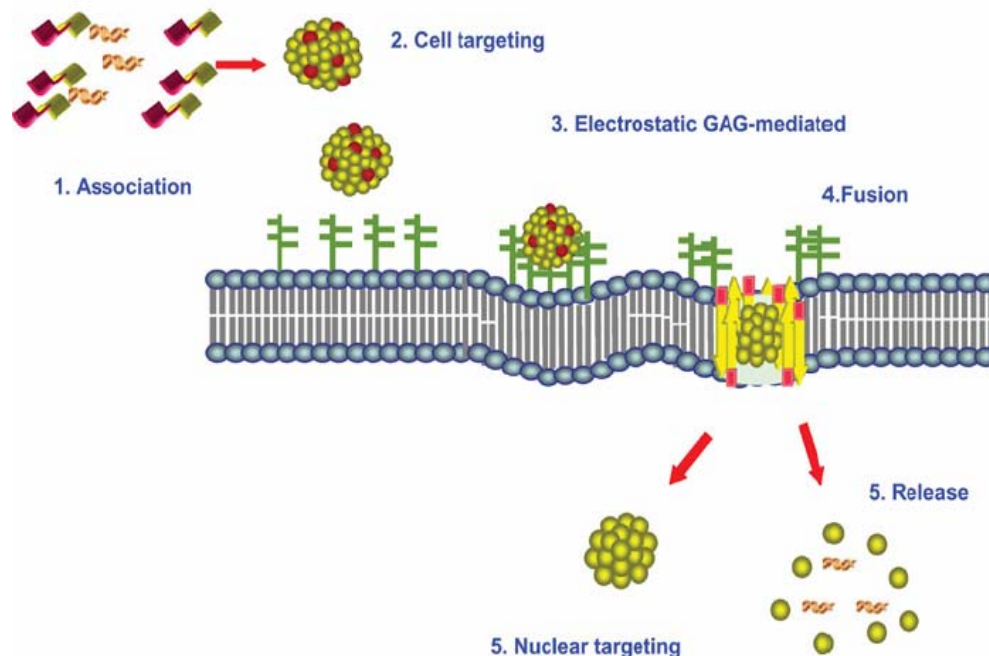


**Figure 3: Mechanism of cellular uptake of MPG–siRNA complexes.**

(1) Formation of the MPG–siRNA complexes through electrostatic and hydrophobic interactions. (2,3) Interaction of the MPG–siRNA complex with the cell surface involving electrostatic contacts with the phospholipid headgroups. (4) Insertion of the complex into the membrane, associated with formation of transient transmembrane  $\beta$ -structures. (5) Release of the MPG–siRNA complex into the cytoplasm or its nuclear targeting. (Crombez et al., 2007b)

(i) formation of the MPG–siRNA complexes through electrostatic and hydrophobic interactions, (ii) interaction of the MPG–siRNA complex with the cell surface involving electrostatic contacts with the phospholipid headgroups, (iii) insertion of the complex into the membrane, associated with formation of transient transmembrane  $\beta$ -structures that temporarily affect the cell membrane organization, and (iv), finally, the release of MPG–siRNA complex into the cytoplasm or its nuclear targeting. These steps are illustrated in the Figure 3 below (Crombez et al., 2007b).

### 1.6.2. Penetratin

Penetratin is a homeodomain-derived peptide. Homeoproteins define a class of transcription factors that bind DNA through a structure of 60 amino acids in length, called the homeodomain. The initial clue that transcription factors can traverse from cell to cell and thus be secreted and internalized by live cells came from the internalization of the homeodomain of Antennapedia (a *Drosophila* homeoprotein) (Christiaens et al., 2002). The homeodomain of antennapedia was shown to translocate through the plasma membrane of cultured neuronal cells, to reach the nucleus and to induce changes in the cellular morphology.

Prochiantz and co-workers in the classical work on penetratin (Le, I et al., 1993; Derossi et al., 1994c) proposed the use of penetratin, corresponding to residues 43–58 of the homeodomain, as a vehicle for the intracellular delivery of hydrophilic cargo molecules like oligopeptides (Theodore et al., 1995), oligonucleotides (Troy et al., 1996) and peptide nucleic acids (PNA) (Derossi et al., 1998).

Penetratin had proven valuable in the transfer of proteins such as those involved in the cell cycle progression and induction of apoptosis. The peptide is efficient for the transfer of small proteins (less than 100 residues), but its efficiency is poorer for larger proteins. Penetratin can also be used for transfection of nucleic acids, such as antisense oligonucleotides, peptide nucleic acids (PNAs) and double-stranded DNAs, with, however, much poorer transfection efficiency for double stranded DNA (Deshayes et al., 2005).

The cellular uptake of penetratin occurs both at 37°C and 4°C, this observation excludes internalization via endocytotic pathway (Derossi et al., 1994a; Derossi et al., 1996b), whereas cellular import of reverse forms of various CPPs suggested that it is a receptor-independent process (Derossi et al., 1996a). The nontoxic penetratin translocates across cellular membranes without membrane damage. There was suggestion of direct interaction of penetratin with membrane. But more persuasive is the proposal that the internalization mechanism of penetratin favours the formation of inverted lipid micelles (Derossi et al., 1994b; Prochiantz, 1996). This view would imply that the peptide remains in an aqueous environment. Such a mechanism would facilitate the transport of hydrophilic compounds linked to the peptide.

### 1.6.3. Tat peptide

The transcription-transactivating (Tat) protein of HIV-1 is a protein of 101 residues which consists of three functional domains: an acidic N-terminal region required for transactivation activity, a cysteine-rich DNA binding domain and a basic domain comparable to a nuclear localization sequence. One main characteristic of the Tat protein lies in its ability to cross the plasma membrane of neighbouring cells (Frankel and Pabo, 1988).

The minimal peptide-promoting membrane translocation was the 49–57 basic domain. The Tat peptide has been used for transfer of a broad variety of macromolecules, such as fusion proteins and nucleic acids. Oligonucleotides have been most often internalized in the form of covalent Tat/oligonucleotide conjugates (Astria-Fisher et al., 2002)].



**Figure 4: Schematic model depicting adult stem cell differentiation.** Uncommitted MSCs undergo two stages, occurring in the stem cell compartment and the committed cell compartment, prior to acquiring specific phenotypes. In the stem cell compartment, multipotent MSCs give rise to a less potent cell population via asymmetric cell division (A), which then generate more precursor cells with less self-renewal capacity and more restricted differentiation potential via symmetric division (S). In the committed cell compartment, these tri- or bi-potent precursor cells continue to divide symmetrically and generate bi- or unipotent progenitor cells with pre-determined cell fate, which eventually give rise to fully differentiated cells. Recent studies also suggest that the fully committed cells are able to dedifferentiate into more potent cells, and acquire a different phenotype under inductive cues (open arrows) (Baksh et al., 2003).

The earliest experimental evidence supporting the existence of MSCs originated from the pioneering work of Friedenstein *et al.*, who first demonstrated that bone marrow derived cells were capable of osteogenesis (Baksh et al., 2003).

MSCs are considered a readily accepted source of stem cells because such cells have already demonstrated efficacy in multiple types of cellular therapeutic strategies, including applications in treating children with *osteogenesis imperfecta* (Horwitz et al., 2002), hematopoietic recovery (Koc et al., 2000), and bone tissue regeneration strategies (Petite et al., 2000). More importantly, these cells may be directly obtained from individual patients, thereby eliminating the complications associated with immune rejection of allogenic tissue. Despite diverse and growing information concerning MSCs and their use in cell-based strategies, the mechanisms that govern MSC self-renewal and multilineage differentiation are not well understood and remain an active area of investigation (Baksh et al., 2003).

Rodriguez and colleagues outlined the requirements that candidate post-natal tissue-specific stem cells must fulfill to be used for the clinical treatment of degenerated or inherited diseases, as the cells being isolated from a large reservoir of an easily accessible source from human, and should in addition meet the following criteria: (a) long-term expansion *in vitro* accompanied by normal karyotype; (b) multilineage potential of a single cell *in vitro*, and (c) capacity for long-term engraftment and tissue regeneration after transplantation into recipients (Rodriguez et al., 2005b).

### 1.7.1. Adult stem cells

A multipotent stem cell is defined as a special kind of cell that has the unique capacity to self renew for indefinite periods that means that stem cells can be extensively expanded *ex vivo*. Multipotent stem cell can be differentiated into many different cell types with appropriate signal or cocktail.

Multipotent stem cells are present in adult tissues. Owing to lack of a specific and universal molecular marker to identify adult stem cells, functional assays are employed to establish the existence of these stem cells in a tissue. The first Adult multipotent stem cells were isolated from adult bone marrow (Jiang et al., 2002). Now they have been identified in many adult tissues. The bone marrow is the most widely used stem cell source but multipotent stem cells have also been identified in skin, blood vessels, muscle and brain. Given the medical implications, identification of adult stem cells has evoked significant excitement. However, stem cells are rare in adult tissues and difficult to isolate and maintain *ex vivo*.

The heterogeneity of adult stem cell's self-renewal and differentiation potential, is attributable to the fact that the MSC pool comprises not only putative "mesenchymal stem cells" but also subpopulations at different states of differentiation (Baksh et al., 2003). For instance, there exist in the bone marrow MSCs a primitive stem cell population (multipotent MSCs), similar to the hematopoietic stem cell system that is capable of

extensive self-renewal and formation of all the differentiated connective tissues, as well as MSCs with different multilineage potential (e.g., quadra-potent, tri-potent, bi-potent, and uni-potent Mesenchymal stem cells) (Baksh et al., 2004). These various multi-potent MSCs have limited self-renewal capacity and give rise to specific cell types with terminally differentiated phenotype. The multi-potent stem cells are eventually depleted from the MSC pool during long-term culture, due to their low frequency in relation to more differentiated MSC phenotypes, present at higher frequency in the primary tissue source (Baksh et al., 2004). This observation establishes a need for a method of maintaining multipotent stem cells during *in vitro* culture expansion.

Strategies employed to this end to enhance and maintain the multilineage potential of MSCs according to Baksh and colleagues, include: culturing cells with specific growth factors, enriching cells prior to initial plating, and/or culturing cells in a non-contact suspension culture configuration, seeding these cells on tissue culture plates at a standard plating density in a minimal essential medium base containing fetal bovine serum (FBS). Within 24-48 hours, non-adherent cells are removed, and the adherent cells are cultured and passaged to expand the MSC population (Baksh et al., 2004).

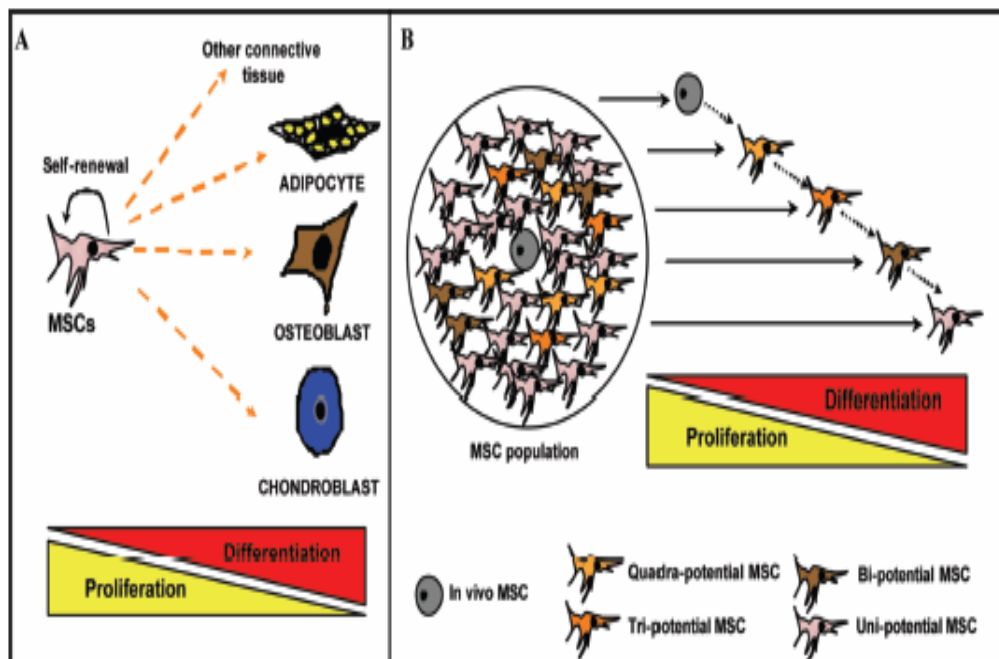


**Figure 5: Models of mesenchymal stem cell differentiation.** (A) In this theoretical model, a mesenchymal stem cell (MSC) has the capacity to differentiate into all connective tissue cell types, including bone, cartilage, tendon, muscle, marrow, fat, and dermis. Furthermore, MSCs have the potential for self-renewal and proliferation and, under defined environmental cues, can commit to a particular differentiation pathway. The lineage-committed cell progresses through several stages of maturation prior to the onset of terminal differentiation, which is marked by the cessation of proliferative capacity and shift toward synthesis of tissue-specific markers, including components of the extracellular matrix. (B) An alternative model illustrating that *in vivo*, MSCs comprise a cell population that consists of mesenchymal cells, which have different differentiation potentials (i.e., quadra-, tri-, bi- and uni-potent). During *in vitro* culture, all or a subset of these mesenchymal cells are isolated. During differentiation, the proliferative potential of these different mesenchymal cells decreases and, depending on the initial state of differentiation, both their proliferative and multilineage potential become limited (Baksh et al., 2004).

### 1.7.2. Human multipotent adipose-derived stem (hMADS) cells

Human adipose tissue is said to contain a population of non-characterized cells, that when harvested by liposuction, are able *in vitro* to undergo adipogenic, osteogenic, chondrogenic, and myogenic differentiation (Zuk et al., 2001b; Zuk et al., 2002).

Rodriguez and colleagues reported that these cells were isolated and characterized from adipose tissue of young donors and are referred to as human Multipotent Adipose-Derived Stem (hMADS). hMADS cells can be maintained *ex vivo* using standard procedure optimized by using an original procedure. (Rodriguez et al., 2004c) hMADS cells reportedly display extensive self-renewal capacity *in vitro*, exhibit a normal diploid karyotype, can withstand freezing/thawing cycles and retain the capacity to undergo differentiation into many mesenchymal cell types, including adipocytes, at the single cell level even after extensive expansion to exhibit characteristics of human fat cells as previously reported by Rodriguez et al. (2004). Within 14 days after induction of adipocyte differentiation, more than 90% of cells accumulate intracellular lipids present as multiple droplet (Rodriguez et al., 2004c).

Rodriguez et al. (2004) showed that immortalized hMADS cells are a unique cell model in displaying the key features of human adipocytes. During the differentiation process, hMADS cells exhibited a gene expression pattern similar to that described for rodent clonal preadipocytes and human primary preadipocytes. Differentiated cells displayed the key features of human adipocytes, i.e., expression of specific molecular markers, lipolytic response to agonists of  $\beta$ -adrenoreceptors ( $\beta$ 2-AR agonist to  $\beta$ 1-AR agonist to  $\beta$ 3-AR agonist) and to the atrial natriuretic peptide, insulin-stimulated glucose transport, and secretion of leptin and adiponectin (Rodriguez et al., 2004a). Compared to other preadipocyte cell lines an important feature of differentiated hMADS cells is their ability to secrete leptin and adiponectin (Rodriguez et al., 2005a). Another distinguishing feature with other preadipocytes is the ability to differentiate into osteoblast and myoblast (Zuk et al., 2001a).

### 1.7.3. Adipocyte differentiation

Adipocytes are known to possess intracrine, autocrine/paracrine, and endocrine properties (Ailhaud, 2000). The adipocyte differentiation program is controlled by the sequential expression of various transcription factors, that is, members of the CCAAT/enhancer binding protein (C/EBP) and peroxisome proliferator-activated receptor (PPAR) Families and the adipocyte determination and differentiation factor-1/ sterol response element binding protein 1c (ADD1/SREBP1c) (Rosen and Spiegelman, 2000).

Differentiation is accompanied by dramatic increases in the specific expression of adipocyte fatty acid binding protein ( $\alpha$ -FABP), and several lipid-metabolizing enzymes [GPDH, glycerophosphate dehydrogenase; FAS, fatty acid synthetase; FAT/CD36, fatty acid transporter; and HSL, hormone-sensitive lipase] and by changes in the expression of cytoskeletal and extracellular matrix proteins (Gregoire et al., 1998). During adipocyte differentiation, the expression levels of types I and III collagen mRNA decrease as preadipocytes lose their fibroblastic characteristics (Weiner et al., 1989). An increase in the levels of type IV collagen, laminin, entactin, and glycosaminoglycans then takes place to form an extracellular basement membrane, which is one of the first ultrastructural changes in the differentiation of adipose cells from precursor cells. (Dani et al., 1989b) showed that  $\alpha$ 2-chain of type VI collagen mRNA is one of the earliest markers of adipocyte differentiation (Dani et al., 1989a). Preadipocyte factor-1, (Pref-1), an epidermal growth factor-repeat (EGF-repeat) containing transmembrane protein, is highly expressed in preadipocytes and its expression is abolished after differentiation to adipocytes (Smas and Sul, 1993a). Pref-1 inhibits adipocyte differentiation and processing of transmembrane pref-1 generates a biologically active soluble form corresponding to the ectodomain (Smas et al., 1997; Smas and Sul, 1993b). Interaction of the EGF repeats of

Pref-1 with still unidentified receptor may mediate the inhibitory effects of Pref-1 in adipocyte differentiation, thereby affecting nuclear events that accompany adipogenesis.

#### 1.7.4. MicroRNAs targeting adipogenesis

MicroRNAs are short (21-22 nucleotides) non coding RNAs, proposed to regulate gene expression at the post transcriptional level. Several hundred miRNAs have been identified in mammals: these have an established role as regulators of genes involved in many key cellular processes including proliferation, differentiation, apoptosis and insulin exocytosis. There is strong evidence for the role of miRNAs as biomarkers of cancer, and there is a growing interest in the role they play in the regulation of glucose homeostasis; specific microRNAs are involved in the regulation of both insulin secretion (miRNA-375) and adipocyte differentiation (miRNA-143).

Despite the known cascade of transcription factors involved in adipogenesis the regulatory network is poorly understood. Although, microRNAs are a novel class of regulators known to be involved in tissue development and diseases, only a few of the more than 500 existing human miRNAs have been assigned a biological function in adipocyte differentiation. In an effort to uncover miRNAs important during adipocyte differentiation, antisense oligonucleotides (ASOs) targeting 86 human miRNAs were transfected into cultured human pre-adipocytes, and their ability to modulate adipocyte differentiation was evaluated by Esau et al. Expression of 254 miRNAs in differentiating adipocytes was also examined on a miRNA microarray (Esau et al., 2004).

Using a combination of expression data and functional assay results Esau and co-workers identified a role for miR-143 in adipocyte differentiation (Esau et al., 2004). miR-143 levels was reportedly increased in differentiating adipocytes, and inhibition of miR-143 effectively inhibited adipocyte differentiation. In addition, protein levels of the proposed miR-143 target ERK5, were higher in ASO-treated adipocytes. These results demonstrate that miR-143 is involved in adipocyte differentiation and may act through target gene ERK5.

Xu and colleagues reported that the deletion of miR-14 in *Drosophila* results in increased levels of triacylglycerol and diacylglycerol, whereas increases in miR-14 copy number have the opposite effect (Xu et al., 2003) Their finding suggests that miRNA might be involved in the regulation of fat metabolism, but the gene that corresponds to *Drosophila* miR-14 has not been found in mammalian genomes.

In line with the observation of Esau and co-workers (Kajimoto et al., 2006d) observed up-regulation of miR-143 in 3T3-L1 cells during adipocyte differentiation. As with the other up-regulated miRNAs, expression of miR-143 was mostly up-regulated at day 9 in kajimoto et al (2006). while Esau et al. (2004) reported as earlier stated that expression of miR-143 was elevated at days 7 and 10 in human adipocytes, but not at days 1 and 4, similar to the observations of kajimoto and co-workers (Kajimoto et al., 2006b; Esau et al., 2004). Esau and colleagues outlined 22 miRNAs differentially expressed in human adipocytes during differentiation. However, Esau's group did not identify similar miRNAs with Kajimoto group, except for miR-143, suggesting that the types of miRNA involved in adipocyte function may differ between human adipocytes and 3T3-L1 cells. The antisense inhibition of miR-10b, 15, 26a, 34c, 98, 99a, 101, 101b, 143, 152, 183, 185, 224, and let-7b, all of which were up-regulated during adipogenesis, did not affect adipocyte differentiation in terms of marker gene expression and the accumulation of lipid droplets. Moreover, the combined inhibition of several miRNAs also did not affect adipocyte differentiation. However, it is possible that more thorough inhibition might be needed to affect differentiation they suggested (Kajimoto et al., 2006c; Kajimoto et al., 2006a).

## 1.8. Objectives

Most drugs are known to target cell surface receptors owing principally to the difficulty of traversing the formidable barrier of the cell membrane to gain access to the cytosolic compartment to deliver bioactive cargo. In the wake of the post-genomic era huge data are currently available in many databases of target predictions of microRNAs and other regulators targeting specific genes responsible for a number of developmental fate decisions, disease processes and metabolic paths-ways that need to be experimentally validated. As such delivery of intracellular cargo is paramount to maximizing the gains and promises of the post-genomic revolution. There are traditionally two methods of delivery system in most laboratories: viral-based and non-viral-based methods. Each of these methods has merits and demerits ranging from poor transfection, cyto-toxicity, low-titers of expression and replication competent retro-viruses. Methods like electroporation lead to poor delivery with marked cell mortality in some cell types. Lipid based transfection agents are equally prone to low transfection efficiency and high cell mortality rates.

Recently, novel classes of peptides have been described, with natural ability to translocate the plasma membrane to access intracellular targets (Derossi et al., 1998). These peptides are known by different names: cell penetrating peptides, trojan horse peptide, membrane permeant peptides and protein-transduction domain.

MPG is a class of these cell penetrating peptides capable of translocating the impervious hydrophilic cell membrane to deliver non-covalently attached cargo. Reports suggest that the use of PTD-based CPPs could be of major importance for therapies against viral diseases or cancers (Deshayes et al., 2005).

This study is aimed at assessing CPP-mediated delivery of FAM-labeled small RNA into mesenchymal stem cells using adherent hMADS cells at different time points, starting from pre-confluent stage, confluent and in adipocyte differentiating stages. The study will evaluate whether MPG translocates hMADS cell membrane to internalize labelled siRNA, cytotoxicity, and transfection efficiency, duration of the cargo in the cell as well as localization of the intracellular cargo.

## 2. MATERIAL AND METHODS

### 2.1. Material

#### 2.1.1. Cell Culture of hMADS cells

Human multipotent adipose-derived stem cells (hMADS) cells were derived from stroma-vascular fraction of human adipose tissue as previously reported (Rodriguez et al., 2004c).

Materials required for proliferation, passaging, and differentiation of hMADS cells include: Dulbecco's MEM low glucose (DMEM) from Biowhittaker, Phosphate Buffer Saline (PBS) (Cambrex), Glutamine (Gibco), Trypsin-EDTA (Gibco) used for detaching adherent cells, HEPES, 100 mm cell culture dishes (Corning), 35 mm dishes (6-well plate) also from Corning, as well as 24-well plates.

#### 2.1.2. Proliferation medium constituents

**Table1. Constituents of Proliferation medium**

Reagents	Company	Final concentration
Fetal Bovine Serum (FBS)	Pan Biotech	10%
Normocin	InvivoGen	0.1 mg/ml
Human Fibroblast Growth Factor 2 (hFGF2)	Sigma	0,0025 µg/ml
Penicillin/ Streptomycin)	Cambrex	100 U+ µg/ml
Glutamine (added every month)	Gibco	2 mM
HEPES	Gibco	10 mM

#### 2.1.3. Differentiation medium constituents

**Table2. Constituents of Differentiation Medium**

Reagents	Company	Final concentration
Ham's F-12	Cambrex	50%
PEN-STREP	Cambrex	100 U+ µg/ml
Human Insulin	Sigma	0,005 mg/ml
Transferrin	Sigma	0.01 mg/ml
T3 (Triiodothyronin)	Sigma	0.0002 uM
Rosiglitazone: (PPAR $\gamma$ agonist),		0.0001 mM
Dexamethasone	Sigma	0.001 mM
IBMX (Isobutylmetaxanthin),	Sigma	0.1 mM

#### 2.1.4. Materials for transfection of hMADS cells

**Table3. Transfection Reagents**

Reagents
N-TER Nanoparticle transfection Peptide (Sigma, Cat # N0538),
N-TER Buffer (Sigma, Cat # N0413),
5', 6-FAM labelled siRNA (sigma)
RNase free water (DEPC-Water)
Phosphate buffered saline (PBS),
Serum- free Medium.

The sequences of the 5'-6-FAM labelled (sense) siRNA (Sigma) were:  
 Scramble sense - GCUCCCUUCAACGCUAAUdTdT  
 Scramble antisense- AAUUAGCGUUGAAGGGAGCdTdT

### 2.1.5. Equipment

**Table 4. Equipment**

Equipment	Company
Sonicating water bath, (420, 35 kHz)	Elma, Transsonic
Microcentrifuge	Roth
Microfuge tubes	Eppendorf
Centrifuge 5702	Eppendorf
MS2 Minishaker	Unilab
Labogaz206	Olympus
CkX 41 Inverted Fluorescence Microscope	Carl Zeiss
Zeiss Axioimager	

## 2.2. Methods

### 2.2.1. Proliferation and Differentiation of hMADS Cells

hMADS cells were thawed, resuspended, and maintained in Dulbecco's modified Eagle's medium (DMEM) pre-warmed to 37°C containing 10% FBS, Penicillin and Streptomycin, Pen/Strep, 100 U+ug/ml, and 0.1mg/ml Normocin (InvivoGen), 10 mM HEPES and L-Glutamine which was enriched every 4 weeks. hFGF-2 was added freshly to the medium for proliferation. The medium was changed every two days until cell reached confluence. After two days of confluence (designated Day 0), cells were then induced to differentiation using Medium II prepared with the reagents listed in Table 1. Three days later, the medium was changed to medium III (lacking DEX and IBMX). Only freshly prepared differentiation media were used. The cells were incubated in standard cell culture conditions, at a temperature of 37°C with air containing 20% oxygen, 5% carbon dioxide and nitrogen. The medium was sterile filtered to avoid contamination. The cells were grown in 10 mm cell culture dishes and sub-cultured into 35mm dish (6-well plate) and 24 well plates during transfection.

### 2.2.2. Preparation of transfection complex and internalization

MPG peptide (N-ter Nanoparticle siRNA Transfection system, Sigma) was thawed at room temperature for 10 mins and sonicated for 5 mins in sonicating water bath (Elma, Transonic) at maximum output and continuous power. This step decreases aggregation tendency of the peptide and can reduce the variability of transfection efficiency. The peptide was then diluted with RNase-free water (DEPC water) as shown in Table 6. To make a stock solution, 2 OD (10.52 nmole) 5'-6-FAM-labeled siRNA (Sigma) was solved in DEPC-water to form 50 µM stock solution, which was further diluted to 5 µM working solution. The 5 µM siRNA working solution was further diluted in MPG buffer as shown in Table 5. The tubes containing the peptide and the siRNA were mixed together, vortexed gently, pulse spinned and incubated at 37°C, for 40 mins to form the siRNA-MPG complex (SMC), as indicated in Tables 5-7, which from now will be referred to as SMC.

This yielded a concentration of 650 nM SMC. The solution was further diluted to appropriate concentration of 30 nM with 0.5x MPG buffer as shown in Table 4. siRNA-only (SO) control was prepared by diluting 14  $\mu\text{l}$  of 5  $\mu\text{M}$  siRNA working solution with 436  $\mu\text{l}$  of 0.5x MPG Buffer, while cell-only (CO) control was formed by mixing 75  $\mu\text{l}$  of MPG buffer and 75  $\mu\text{l}$  RNase free water and diluting with 300  $\mu\text{l}$  of 0.5x MPG Buffer.

**Table 5: Dilution of 5  $\mu\text{M}$  siRNA working solution in MPG Buffer**

Reagent	Tube1A siRNA	Tube2A Cells only control
5 $\mu\text{M}$ siRNA ( $\mu\text{l}$ )	39	
MPG Buffer ( $\mu\text{l}$ )	111	75
Final volume ( $\mu\text{l}$ )	150	75

**Table 6. Dilution of MPG in water**

Reagent	Tube 1B	Tube 2B
MPG ( $\mu\text{L}$ )	24	0
Water ( $\mu\text{L}$ )	126	75
Final volume ( $\mu\text{L}$ )	150	75

**Table 7: Dilution of SMC in 0.5x MPG Buffer**

Reagent	[siRNA] <sub>final</sub> (nM)				
	30	20	10	5	2.5
siRNA-MPG Complex ( $\mu\text{L}$ )	111	74	37	18	9
0.5x MPG Buffer ( $\mu\text{L}$ )	339	376	413	432	441

### 2.2.3. Preparation of 0.5x MPG Buffer

This was prepared by diluting 1500  $\mu\text{l}$  of MPG Buffer in 1500  $\mu\text{l}$  of RNase-free water to make 3000  $\mu\text{l}$  of the buffer for diluting the SMC as shown in Table3.

### 2.2.4. Transfection

Human multipotent adipose derived stem cells (hMADS) grown to stage (80%), 100% confluence as well cells in Day 3 of differentiation into adipocytes differentiation at Day 3 (D 3), and cell in Day 10 after adipocytes (confirmed by Oil-Red-O staining) D10 on a glass coverslip (Corning) which was sterilized by dipping in 70% ethanol and in turn drying in bunsen burner flame, in a 6 well plate or 24 well plate were washed with PBS and then transfected with the diluted SMC, SO and CO to the respective wells, and allowed to incubate for 3-5 mins at room temperature and thereafter equal amount of serum and antibiotic free DMEM medium was added and allowed to incubate for 4hrs at standard cell culture condition at 37°C, 5% CO<sub>2</sub>. After this incubation, complete medium was added and allowed to incubate for 24h, 48h, and 72h. The cells were processed for fluorescence microscopy by fixing them in 3.7% formaldehyde for 10 mins, counter-stained with DAPI and mounted on a slide as described below.

### 2.2.5. Slide Preparation for Fluorescence microscopy

The coverslip containing the transfected cells were carefully detached from the wells and Rinsed in 2 changes of PBS, avoiding keeping the cells long in the PBS to prevent

detaching of the adherent cells from the coverslip. The cells were fixed in 3.7% formaldehyde (prepared by diluting 10 x stock in PBS.) for 10 mins in a shaker at room temperature. The cells were washed in 2 changes of PBS for 5 mins and counter stained with 0.05 ng/  $\mu$ L 4',6-diamidino-2-phenylindole (DAPI) for 5 mins. DAPI stains the nucleus blue. They were washed in PBS for 5 mins, after which the coverslips were mounted on clean slides in PBS or vector-shield and sealed with sealant. PBS was mostly used since, mounting in vector-shield leads to the fading of the blue staining of DAPI after long exposure. The slides were then observed using Axioimager, Epifluorescence microscope (Zeiss), using FAM and DAPI and phase contrast channels.

### 2.2.6. Fluorescent microscopes

Two fluorescent microscopes were used in this study. The Zeiss Axioimager and Olympus CKX 41 inverted microscopes with reflected fluorescence system. The later was used for routine cell culture microscopy.

### 2.2.7. Zeiss Axioimager epifluorescence microscope

The Zeiss Axioimager is a wide-field epifluorescence microscope. It is a versatile upright system that can visualize a wide variety of fluorophores. The system is controlled using MetaMorph software according to the manufacturer's manual. Images are captured on a sensitive CCD camera. It is used for visualizing fluorescent probes in cells and immunofluorescence with thin specimens. Images were taken in 4',6-diamidino-2-phenylindole (DAPI) channel which excites at 359 nm and emits at 461 nm. DAPI was used to detect the nuclei in blue channel. 6-carboxy fluorescein (FAM) excitation is at 494 nm and fluorescence emission is at 518 nm. FAM was used to detect the siRNA in green channel.



Figure 6. Zeiss Axioimager. [www.mbfbioscience.com/](http://www.mbfbioscience.com/)

### 2.2.8. Oil -Red-O Staining

Oil-Red-O is a lipophilic diazo red dye that stains intracellular lipid droplets red. It was prepared as previously described (Massiera et al., 2003)

0.5 g Oil-Red-O was dissolved in 100 ml Isopropanol and stored at 4°C to make a stock solution. 18 ml stock solution was diluted in 12 ml milliQ water (MQ) or deionized water giving a 30 ml final working solution. The resulting solution was filtered using whatman filter paper.

Cells were washed in PBS twice and fixed in 10% formaldehyde (in PBS) for 15 min at room temperature. The fixative was removed and replaced with filtered Oil-Red-O solution and incubated for 1 h at room temperature. After staining, the cells were washed thoroughly with PBS until excess stains were removed. Mature adipocytes containing lipid droplets stained red.

### 3. RESULTS

#### 3.1. hMADS cells adipocyte differentiation

The hMADS cells were grown to confluence and induced to adipocyte differentiation on Day 0. The fibroblast-like morphology was visible before Day 0, which was the day of induction (Figure 7 A) and Day 1 (B), but from Day 3 (C) there was remarkable change in morphology of the cells. The cell morphology gradually became oval with numerous globular shaped fat droplets. By Day 8 (D), Day 10 (E), and Day 15 (F) differentiated fat cells were apparent with clusters of fat droplets. Oil-Red-O staining also confirmed the presence of fats cells as indicated by the red staining of the cells that developed fat droplets (G,H and I). The intensity of red staining which is a measure of degree of differentiation into fat cells increased from Day 8 through Day 10 and became much more intense by the fifteenth day (Day 15) as shown by Figure 7 ( G,H,I,J).

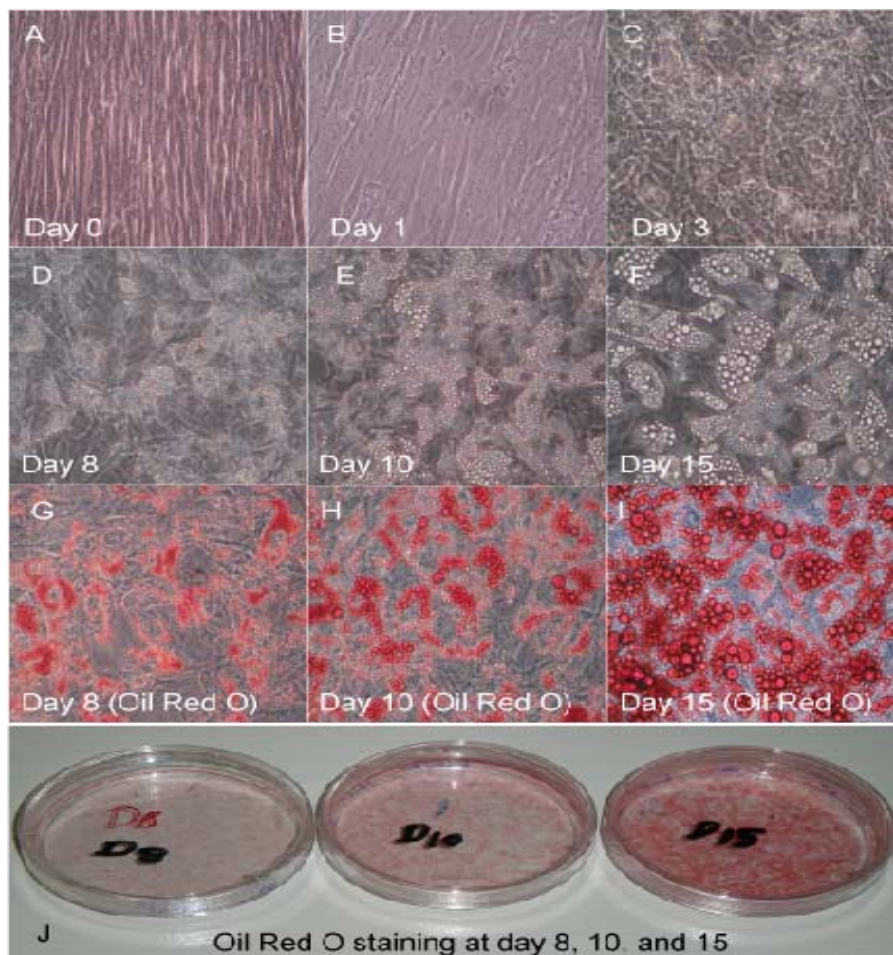


**Figure 7:** Differentiation of hMADS cells. hMADS cells were grown to confluence and induced to adipocyte differentiation on Day 0. The fibroblast-like morphology seen Day 0 (A) and Day 1 (B), From Day 3 (C) cell morphology gradually became oval with numerous globular shaped fat droplets that increased in size and in number as differentiation progressed from Day 3, Day 8 (D) through Day 10 (E) and to be come fully matured adipocytes in Day 15 (F). Oil-Red-O staining of the cells at time points Day 8 (G), Day 10 (H) and Day 15 (I) with pictures of dishes showing increasing staining intensity from Day 8 to Day 15 (J).

### 3.2. MPG-mediated siRNA delivery into hMADS cells

MPG-mediated delivery was investigated in confluent and in differentiating of hMADS cells. Cells were grown on cover-slips and they were transfected for 4h with a 15 nM concentration of SMC for pre-confluent stage and 30 nM for confluent and adipocyte differentiating hMADS cells. The incubations were for 24h, 48h, and 72h post-transfection as the case may be. The viability of the cell was investigated and results shown below. Delivery of siRNA into hMADS cells were also investigated with regards to localization of the siRNA and the results are presented below.

### 3.3. Viability after MPG-mediated siRNA delivery

#### 3.3.1. Does the transfection of pre-confluent cells with SMC affect cell viability?

In order to investigate the above, hMADS cells were transfected with 15 nM of SMC for 4h and examined with Axioimager after 48h of incubation (Figure 8 upper panel: A,B,C). No cell mortality was observed in the SMC transfected cell. No evidence of cytotoxicity was observed in the SMC SO, and CO. The cells overlaid with the free siRNA, SO (B) and the cells overlaid with cell only (CO) containing the MPG buffer alone (C,F,I) showed virtually similar cell morphology and structure with the cells transfected with SMC. There was no evidence to suggest that there was any morphological variation in cells attributable to the complex. These results suggest that the MPG was not toxic to hMADS cells within the investigated concentration.

#### 3.3.2. Transfection of confluent and differentiating hMADS cells with siRNA-MPG complex (SMC) does not affect cell viability

Confluent (Figure 3 middle panel: D,E,F) and adipocyte differentiating hMADS cells (Figure 3 lower panel, G,H,I) were transfected with 30 nM of SMC for 4h and examined with Axioimager after 48h of incubation. There was no evidence to suggest. There was no morphological variation in cells attributable to the complex. There was no mortality of the cells. The cells overlaid with the free siRNA (E,H) and the cells overlaid with cell only (CO) (right panel, F,I) showed virtually similar cell morphology and structure with SMC transfected cells (D,G).

The cell morphology of the SMC and SO and CO were virtually similar in cell content. There was no distortion or detachment of the adherent cells that could be directly linked to SMC. There was no evidence of cell mortality associated to the MPG transfection. There was comparable morphology and cell architecture in the SMC, SO and CO as indicated by Phase contrast images of the confluent and the differentiated cells. There was also no indication that the MPG interfered with the differentiation process. MPG showed no adverse effect on hMADS cells viability. This result suggests that MPG was mild to the hMADS cell, and as such does not adversely affect the viability of hMADS cells within the investigated concentration.

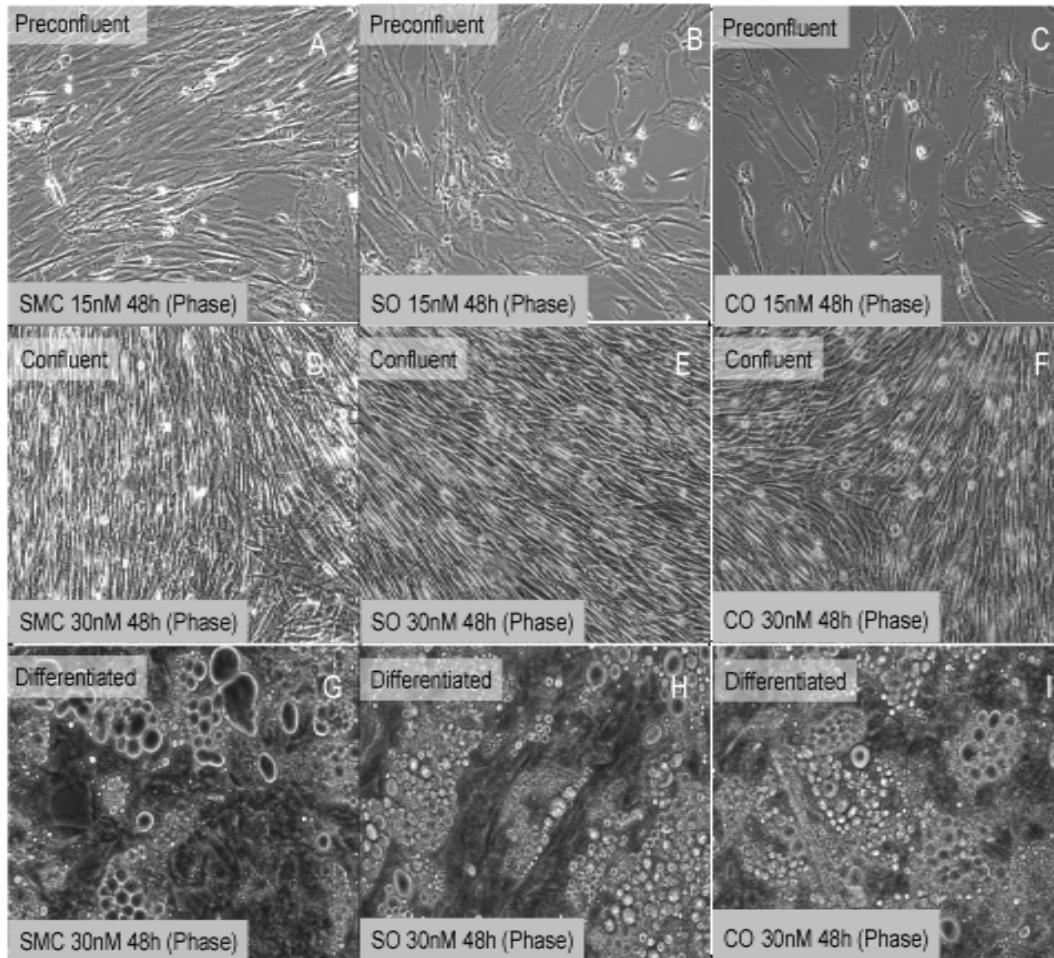
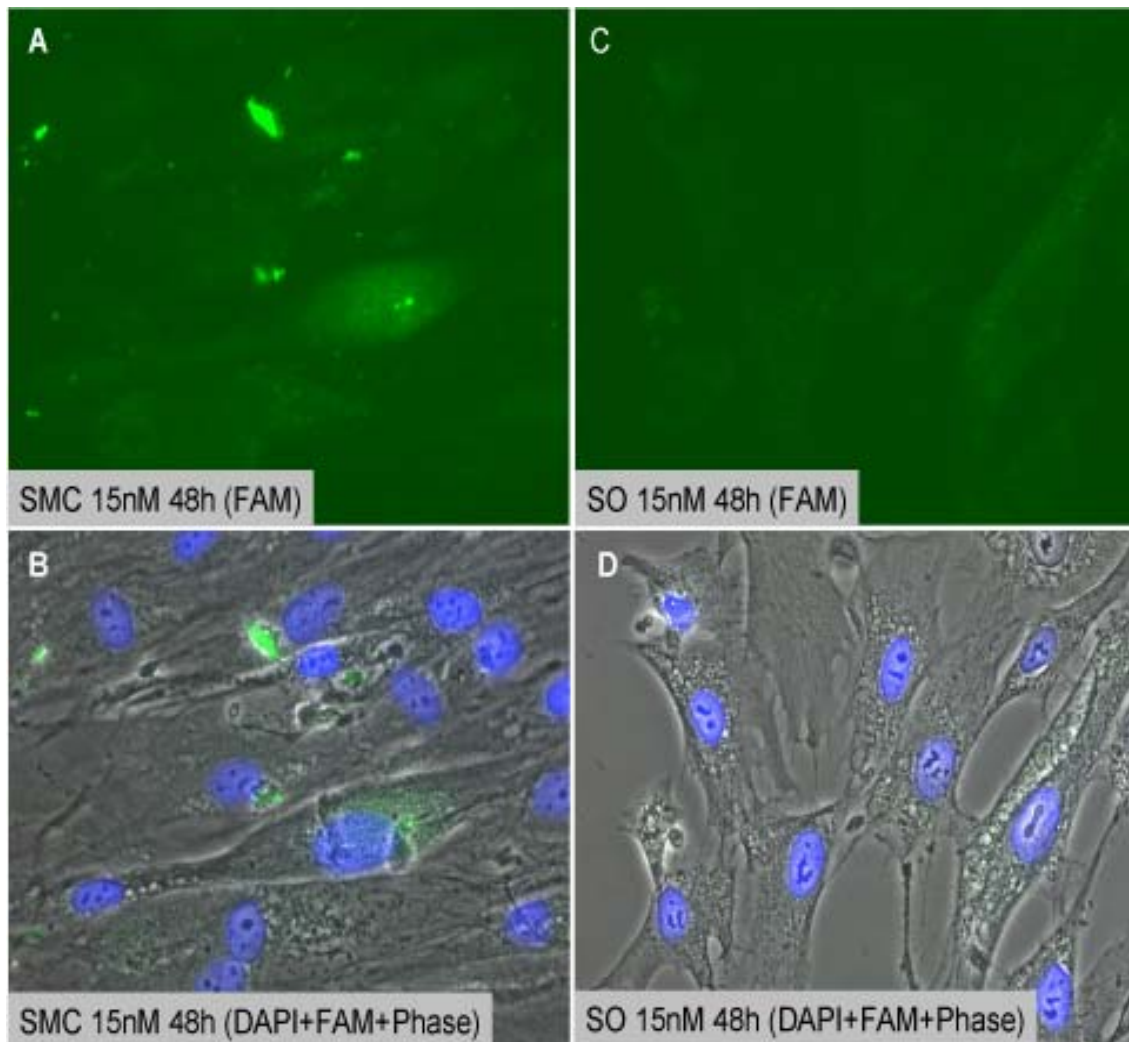


**Figure 8: Cell viability test.** Phase contrast images of hMADS cells transfected with SMC and overlaid with free siRNA, SO and cell only, CO at concentration of 15nM for the pre-confluent time point (A,B,C), 30 nM for the confluent (D,E,F) and Differentiated stages (G,H,I), 48h post-transfection. There was no visible adverse morphological variation between the peptide treated cells (left panel: A,D,G), free siRNA, SO (middle Pane, B,E,H) and the cell only (CO) (right panel: C,F,I), in both the differentiated and undifferentiated stages. There was no evidence to suggest that MPG adversely affected differentiation of hMADS cells to adipocytes as there were differentiated cells with oval shaped lipid droplets in both SMC transfected and the cell only control (lower panel). This suggests that the SMC transfection does not lead to cell mortality in hMADS cells at the evaluated concentration.

### 3.3.3. Transfection of pre-confluent cells

Since hMADS cells are hard to transfect (Zaragosi et al., 2007b), transfection of hMADS cells were undertaken to find out whether SMC could penetrate hMADS cells to deliver labeled double stranded siRNA cargo. Figure 9, 10, and 11 illustrate the results obtained. To investigate whether MPG could deliver labeled double-stranded siRNA into hMADS cells, 50% confluent hMADS cells were transfected for 4h with 15nM of SMC and overlying the controls with free FAM labeled-siRNA and cell only control consisting of MPG buffer ( which served as control for cell viability and toxicity evaluation) after 24h and 48h showed that MPG efficiently delivered the FAM-labeled siRNA across the membrane into the cytoplasm and in some cases into the nucleus or at the nuclear membrane of the the treated hMADs cells. But MPG here showed dotted or punctuated fluorescent speckle within the cells transfected with SMC (Figure 9 A, B and 10 C, D). The control group overlaid with free siRNA did not show these green fluorescent speckles. The same

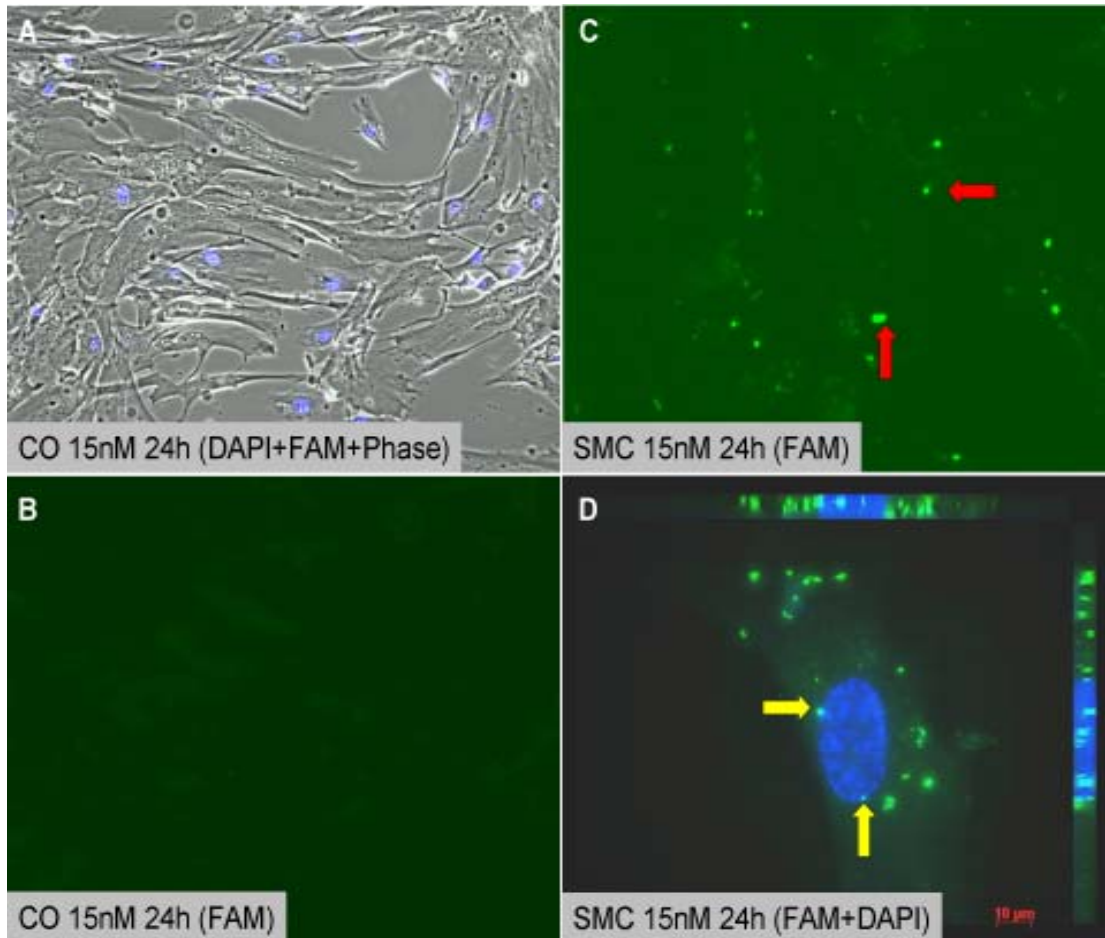
observation was true for the cell only (CO) control group which did not have the speckle. However, there was background green fluorescence in the control sometimes highlighting the cell inside, which was instructive in determining whether the fluorescence was inside or outside the cell.



**Figure 9:** Fluorescence microscopy analysis 48h after transfection of pre-confluent hMADS cells. Cells were transfected for 4h with 15 nM siRNA-MPG complex (SMC), (A and B). Control experiment (C,D): cells were overlaid for 48 h with free siRNA only. FAM channel (A, C) merged image of FAM, DAPI, and Phase contrast channels (B, D), nucleus was stained with DAPI (blue). Images were acquired with Zeiss Axioimager. Abbreviations: SMC; siRNA-MPG complex, SO: siRNA only, FAM: 6-carboxy fluorescein, DAPI: 4',6-diamidino-2-phenylindole.

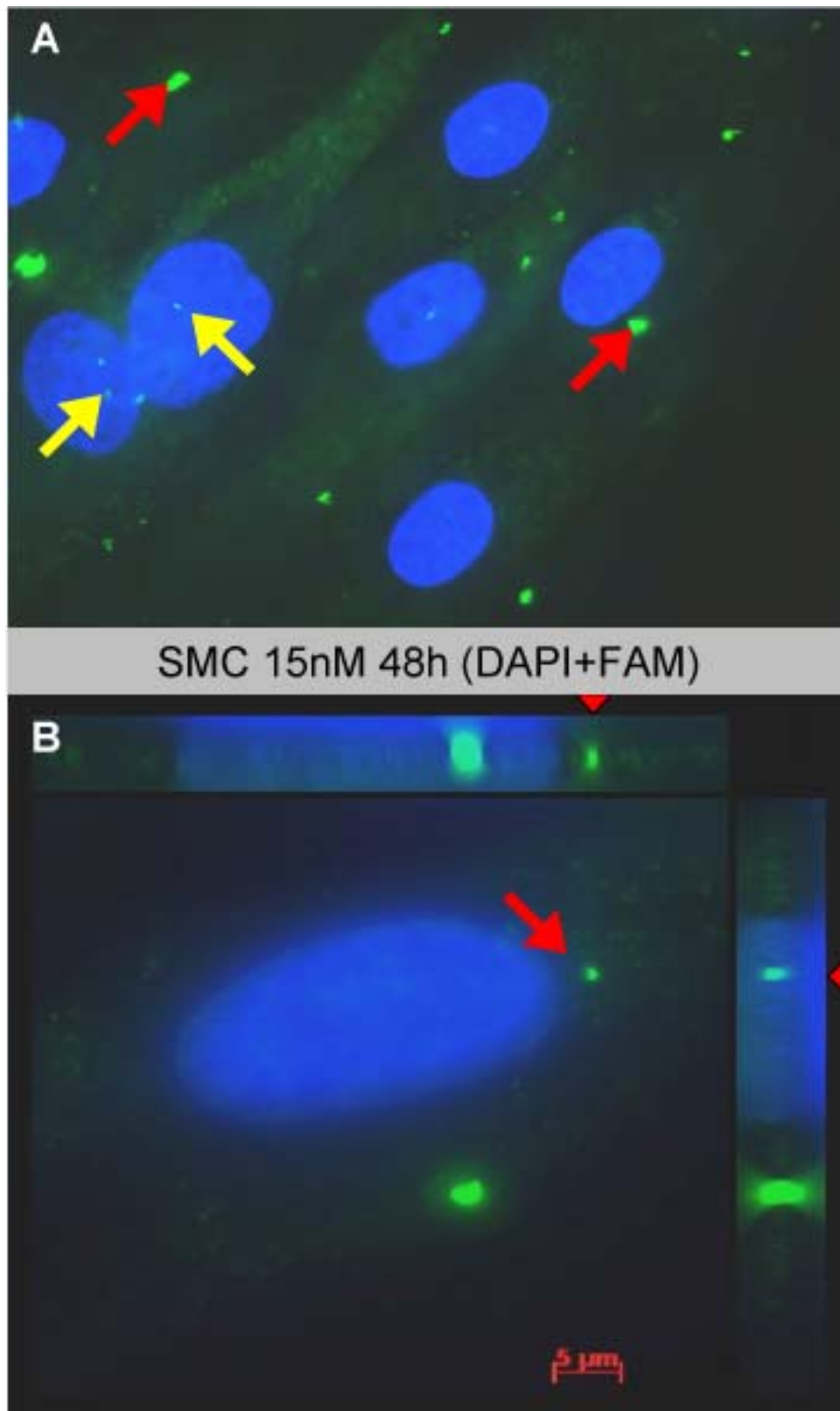
In Figure 10, pre-confluent hMADS cells were transfected for 4h with 15 nM, 5'-6-FAM labeled siRNA-MPG complex (C, D). Control cells were overlaid for 4h with cell only control composed of MPG buffer (A, B). In (A) blue staining nuclei were apparent but with no fluorescent speckles as seen in C and D. Image B in FAM channel, contrary to C did not show the bright speckles but highlighted the background outlines of the cells. Therefore in C and D the bright green speckles showed the labeled siRNA construct. In D the MIP showed the speckle at the nuclear membrane as well as within the cytoplasm.

The punctuate speckles were exclusively detected in the SMC cells indicating internalization of the siRNA by MPG.



**Figure 10:** Fluorescence microscopy analysis 24h after transfection of pre-confluent hMADS cells. Cells were transfected for 4h with 15 nM, 5' 6-FAM labeled siRNA-MPG complex (C, D). The bright green punctate speckles show the labeled siRNA construct. They are seen more pronounced in FAM channel in the SMC (C, D). MIP (D) showed the speckles at the nuclear membrane (yellow arrow) as well as cytoplasm (red arrow). Control cells were overlaid for 4 h with cell only control composed of MPG buffer (A, B). Control experiment: (A merged image of DAPI, FAM, and Phase) and B (FAM). The blue stained nucleus were apparent but with no fluorescent speckles (A) as in C and D which can be confirmed in Image B to be absent. The background outlines of the cells were also visible in B but no fluorescent speckle. The nucleus was counter stained with DAPI. Abbreviation: SMC: siRNA-MPG complex, SO: siRNA only, FAM: 6'-carboxy fluorescein, DAPI: 4',6-diamidino-2-phenylindole, MIP: Maximum intensity projection.

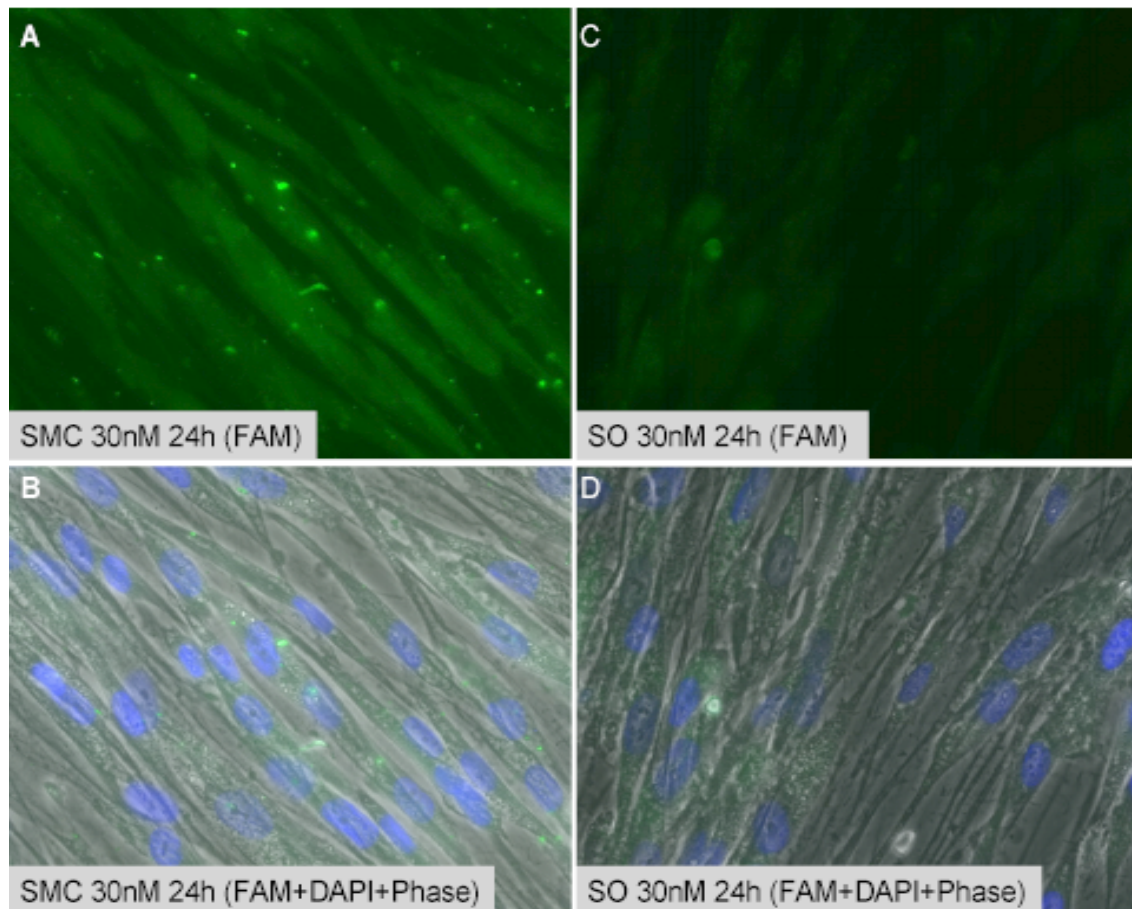
In Figure 11, pre-confluent cells were transfected for 48h with 15 nM siRNA-MPG complex. The image A shows bright green punctate speckles or spots in 90% of the cells in the shown field of view. B) Maximum intensity projection MIP, of the fluorescent speckles (red arrow) lie at the plane of the nucleus within the cytoplasm.



**Figure 11:** Fluorescence microscopy analysis 48h after transfection of pre-confluent hMADS cells. A) Cells were transfected for 4h with 15 nM siRNA-MPG complex. The image shows bright green speckle in 90% of the cells in the shown field of view. (B) Maximum intensity projection MIP, of the fluorescent speckles (red arrow) lie at the plane of the nucleus within the cytoplasm. Nucleus was counter-stained with DAPI. SMC: siRNA-MPG complex, SO: siRNA only, FAM: 6- carboxy-fluorescein. DAPI: 4',6-diamidino-2-phenylindole.

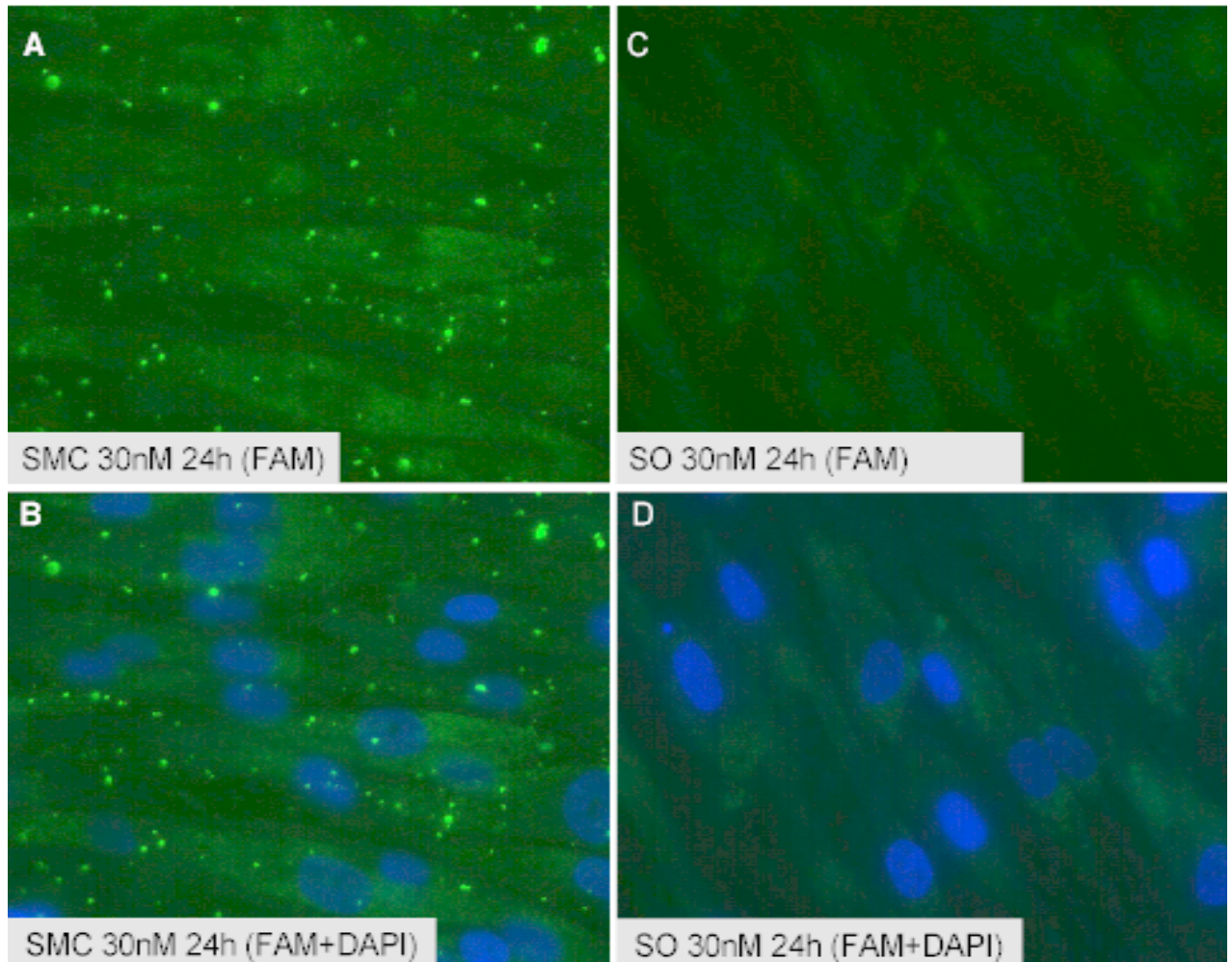
### 3.3.4. Transfection of confluent cells (24h post-transfection)

The hMADS cells are known to be hard-to-transfect (Zaragosi et al., 2006). This prompted the evaluation of transfection of confluent hMADS cells using MPG. The transfection of confluent hMADS was performed for 4h and examined with Axioimager 24h, 48h, and 72h post-transfection using concentration of 30nM SMC, while the control groups were overlaid with free FAM-labeled siRNA (SO) and Cell only (CO). Figures 12, 13, and 14 show transfection after 24h. There were strong punctuated fluorescent speckles detected in SMC transfected cells in about 80 % of (Figure 12 A, B) and 95% of the cells (Figure 13 A, B). The pattern of distribution of fluorescence was similar to the pattern observed in the pre-confluent cell stage. Which presented spotted or punctuate, non-homogenously distributed fluorescent appearance.



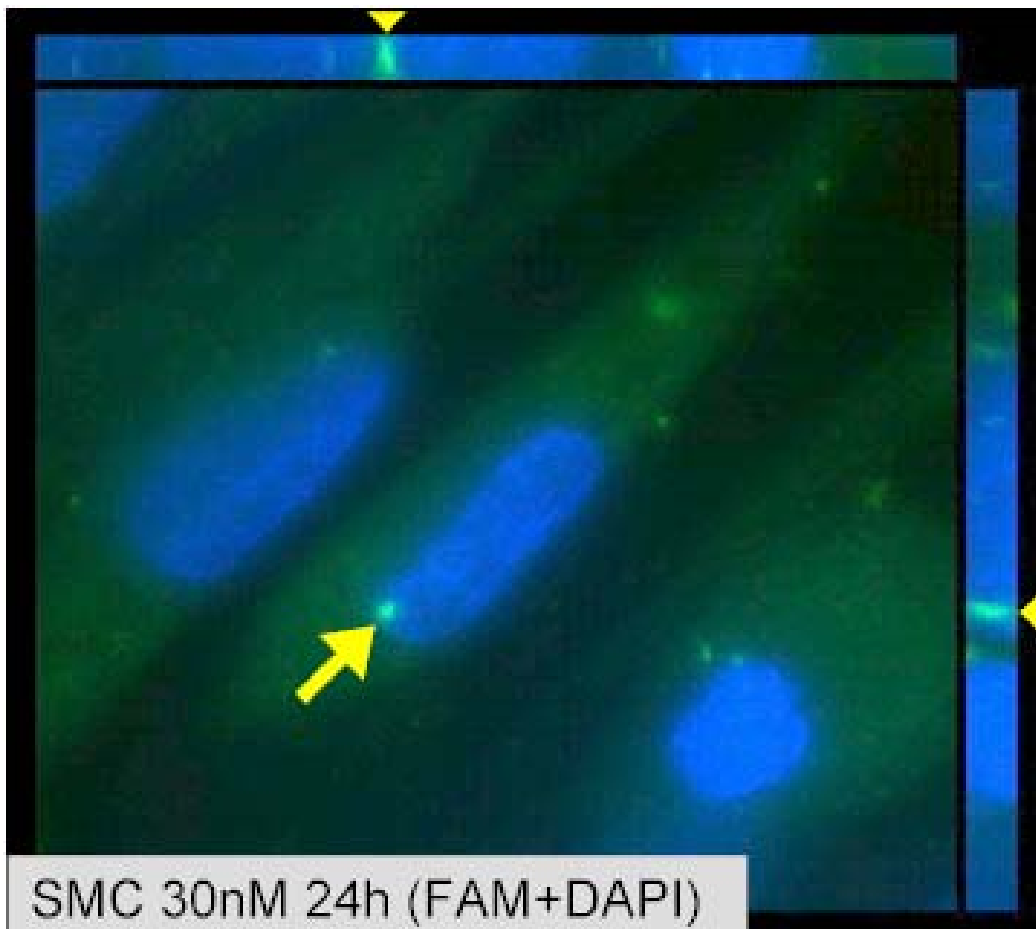
**Figure 12:** Fluorescence microscopy analysis 24h after transfection of confluent hMADS cells. Cells were transfected for 4h with 30 nM siRNA-MPG complex (A and B). Bright punctuate fluorescent speckles were seen in cytoplasm in 95% of the cells (A and B). Control experiment: cells were overlaid for 4 h with free siRNA only (C and D). There was no fluorescent speckle present in the SO; however the cell background was visible. FAM channel (A and C) and merged images (B, D). Nucleus was stained with DAPI (blue). SMC: siRNA-MPG complex, SO: siRNA only, FAM: 6'-carboxy fluorescein, DAPI: 4',6-diamidino-2-phenylindole.

Figure 13 shows the image of SMC transfected cells 24h after transfection (A). The DAPI and FAM images (lower panel) revealed that there were numerous punctuate fluorescent speckles seen in A in more than 95% of the cells. Compared to the control (Figure 13, C, D), there was no fluorescent speckle detected.



**Figure 13:** Fluorescence microscopy analysis 24h after transfection of confluent hMADS cells. Cells were transfected for 4h with 30 nM siRNA-MPG complex (SMC) (A and B). There were numerous Punctuate fluorescent speckles seen in A (FAM channel) and B (Merged DAPI and FAM channels) in more than 95% of the cells. Control experiment: cells were overlaid for 4 h with free siRNA only (C,D).The control showed no fluorescent speckle. FAM channel (C) and merged DAPI and FAM channels (D). The nucleus was counter-stained with DAPI (blue). SMC: siRNA-MPG complex, SO: siRNA only, FAM: 6- carboxy fluorescein. DAPI: 4',6-diamidino-2-phenylindole.

To show that the fluorescence speckles were localized in the nucleus of the cell the maximum intensity projection image at the plane of the nucleus showed localization of the fluorescence within the nucleus (yellow arrow). The speckles were high-lighted by the yellow arrow in the nucleus, indicating that the speckles lie within the nucleus which might suggest nuclear delivery of the labeled siRNA (Figure 14).



**Figure 14:** Fluorescence microscopy analysis 24h after transfection of confluent hMADS cells with 30nM SMC. Maximum intensity projection (MIP) of the fluorescent speckle (yellow arrow) of labelled SMC lies within the nucleus indicating also nuclear localization of the siRNA construct. siRNA was FAM -labeled and nucleus stained with DAPI. SMC: siRNA-MPG complex, SO: siRNA only, FAM: 6-carboxy fluorescein DAPI: 4',6-diamidino-2-phenylindole

### 3.3.5. The siRNA-MPG complex was able to deliver siRNA into confluent hMADS cells (48h post-transfection analysis)

To assess the ability of MPG to deliver siRNA into confluent hMADS cells, the cells were transfected for 4h with 30 nM SMC and control overlaid with SO for 4h. They were examined 48h post-transfection using Axiomager. Figure 15 (A) depicts the SMC in FAM channel (A) and the merged image of FAM, DAPI and Phase contrast (B). Punctuated fluorescence speckles were observed in the SMC within the cytoplasm, but there seem to be fewer cells retaining the fluorescent speckles (however the intensity of the speckles seems to be weaker but cell boundaries were clearly visible).

In the control Figure 15 (C and D), no fluorescence was observed in the control SO. The results showed that MPG could deliver labeled siRNA into the cytoplasm and nucleus of confluent hMADS cells 48h post-transfection.

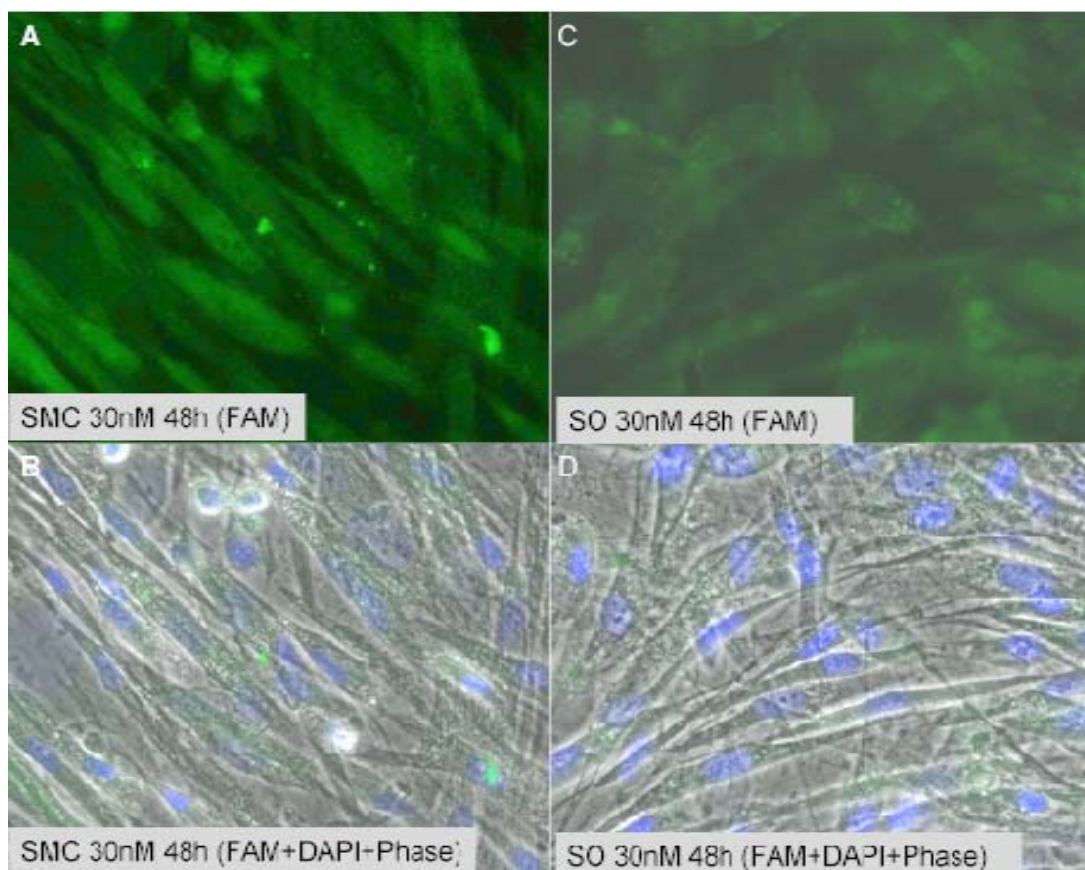


**Figure 15:** Fluorescence microscopy analysis 48h after transfection of confluent hMADS cells. Cells were transfected for 4h with 30 nM siRNA-MPG complex (A and B). Punctuate fluorescent speckle were seen in cytoplasm of the cells but they appear fewer in number (A and B). Control experiment (C and D): cells were overlaid for 4 h with free siRNA only. There was no fluorescent speckle present in the SO; however the cell background was visible. FAM channel (A and C) and nucleus was stained with DAPI (blue). Nucleus was stained with DAPI (blue). SMC: siRNA-MPG complex, SO: siRNA only, FAM: 6'-carboxy fluorescein, DAPI: 4',6-diamidino-2-phenylindole.

### 3.3.6. Transfection of confluent cells (72h post-transfection analysis)

The same observation for 48h was made for the 72h post-transfection, the fluorescent speckles were observed in Figure 16, 72h post-transfection of confluent hMADS cells with 30 nM SMC, SO and CO. However, the observed speckles were fewer and more diffused within the cytoplasm (making the cell structure to glow revealing their boundaries) than those observed 24h post-transfection but like in 48h, the cell outlines were very apparent showing more defined cell boundaries.

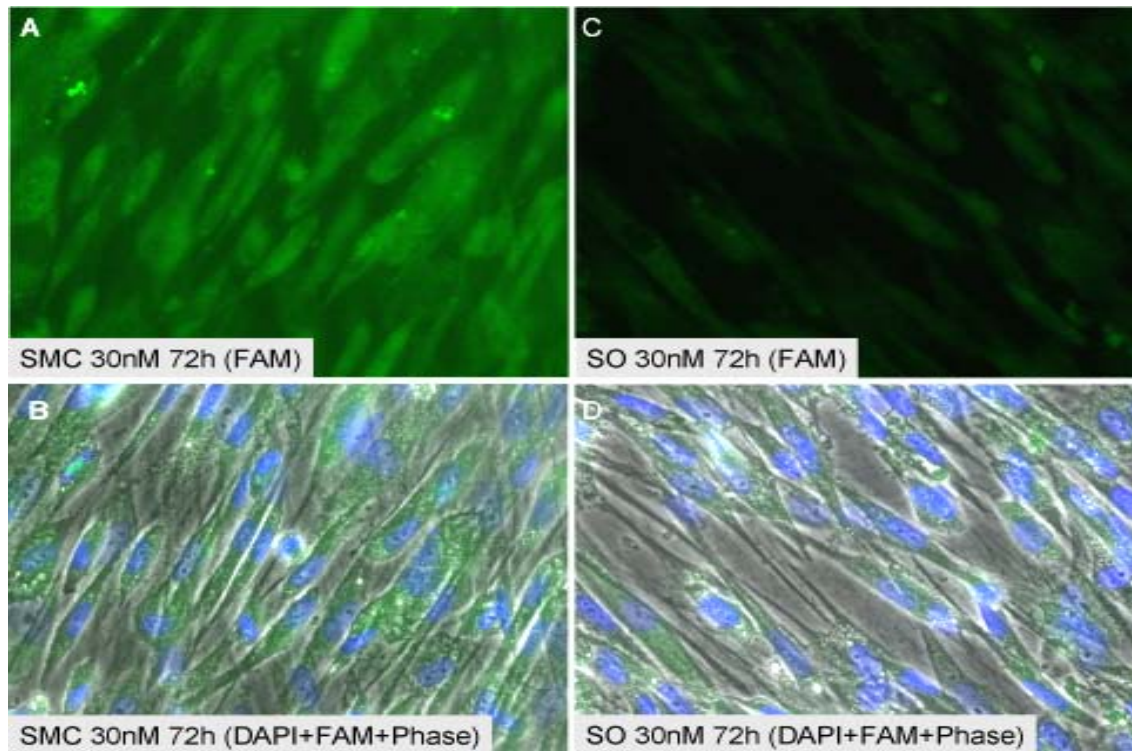


**Figure 16:** Fluorescence microscopy analysis 72h after transfection of confluent hMADS cells. Cells were transfected for 4h with 30 nM siRNA-MPG complex (A and B). Punctuate fluorescent speckle were seen in cytoplasm of the cells. (A and B). Control experiment (C and D): cells were overlaid for 4 h with free siRNA only. There was no fluorescent speckle present in the SO; however the cell background was visible. FAM channel (A and C) and nucleus was stained with DAPI (blue). Nucleus was stained with DAPI (blue). SMC: siRNA-MPG complex, SO: siRNA only, FAM: 6'-carboxy fluorescein, DAPI: 4',6-diamidino-2-phenylindole.

In Figure 17, the Maximum intensity projection, MIP image indicates that fluorescent speckles were seen in the cytoplasm (red arrow) and nucleus (yellow arrow) indicating that the speckle representing the labeled SMC lies within the nucleus and cytoplasm at the plane of the nucleus. Despite the weakening fluorescence observed 48h and 72h post-transfection, using the Olympus inverted microscope fluorescent system, fluorescence were detected in the SMC transfected group up to 6 days post-transfection (data not shown).

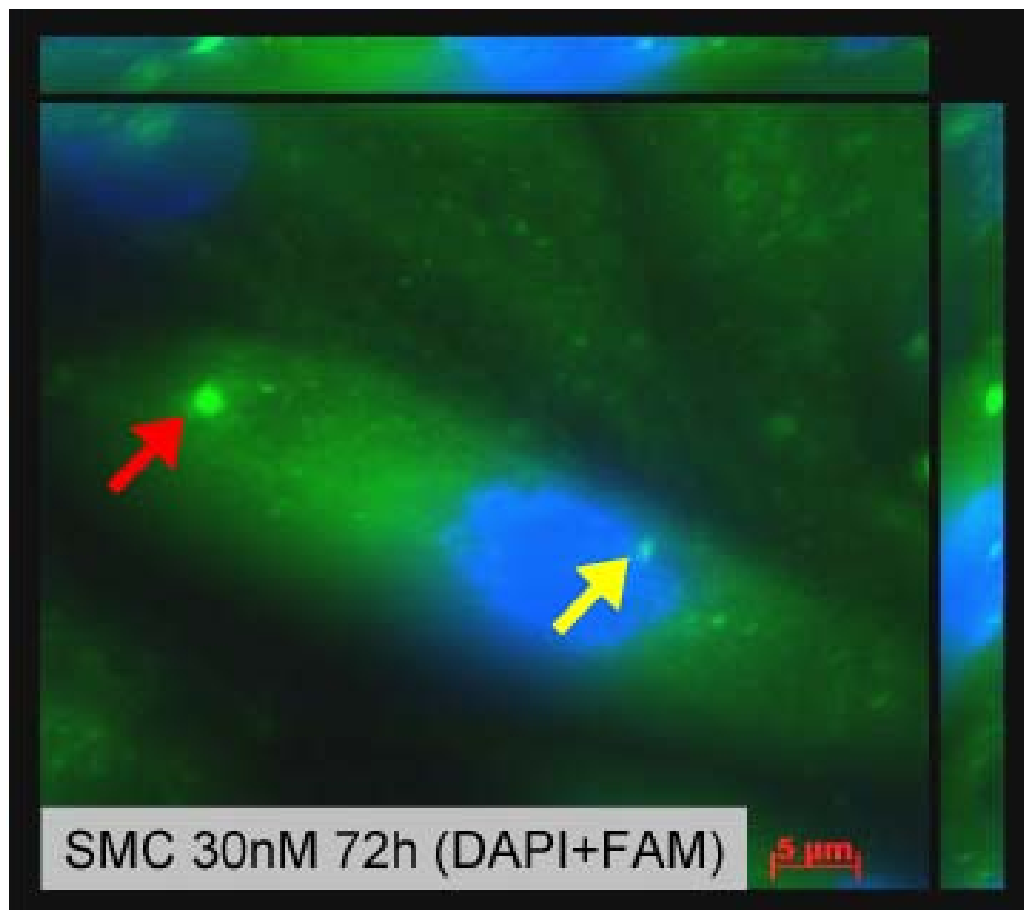


**Figure 17:** Fluorescence microscopy analysis 72h after transfection of confluent hMADS cells with 30nM SMC. Maximum intensity projection (MIP) of the fluorescent speckles were seen in the cytoplasm (red arrow) and nucleus (yellow arrow) indicating that the speckle representing the labelled SMC lies within the nucleus and cytoplasm at the plane of the nucleus. siRNA was FAM-labeled and nucleus was stained with DAPI (blue). SMC: siRNA-MPG complex, SO: siRNA only, FAM: 6- Carboxy- Fluorescein DAPI: 4',6-diamidino-2-phenylindole.

### 3.3.7. Transfection of differentiating cells at Day 3

Having observed punctuate fluorescent speckles of siRNA-MPG complex in the cytoplasm and the nucleus in confluent cells, hMADS cells were differentiated and transfected on Day 3 after induction to see whether a reproducible result will be obtained in the differentiating cells. Transfection was done with 30nM SMC, and overlaid with SO and CO, for 4h. The result was consistent with that observed in the pre-confluent and confluent stages, as indicated below.

After 24h post-transfection of differentiating hMADS cells at Day 3, there was evidence of punctuate speckles of the 5'-labeled siRNA by the MPG complex at the concentration of 30nM SMC. The Maximum intensity projection MIP (Figure 18), of the fluorescent speckle of the labeled SMC were seen localized in the cytoplasm (red arrow) indicating that the speckles localized in the cytoplasm and the yellow arrows point at the speckle in the nucleus. This demonstrated that MPG was able to deliver siRNA into the cytoplasm and nucleus of differentiating hMADS after 24h Post transfection.

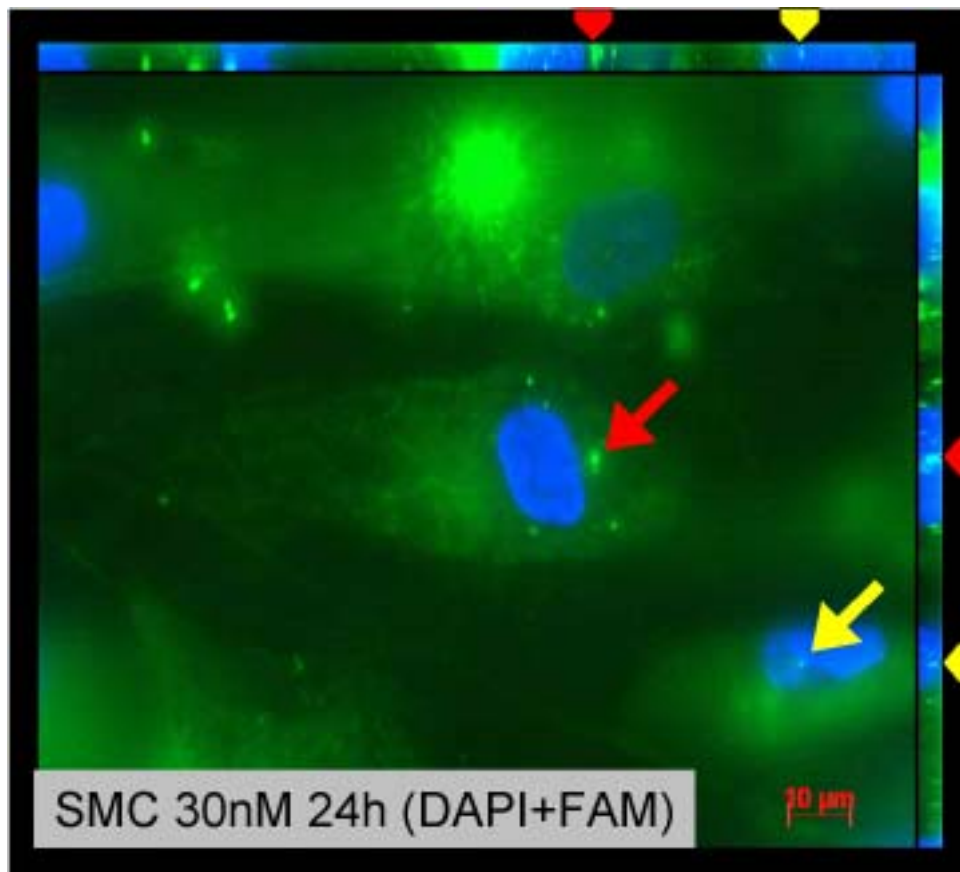


**Figure 18:** Fluorescence microscopy analysis 24h after transfection of differentiating hMADS cells at Day 3. Maximum intensity projection MIP, of the fluorescent speckles were seen in the cytoplasm (red arrow) and nucleus (yellow arrow) indicating that the punctuate speckles of SMC lie within the nucleus and cytoplasm at the plane of the nucleus. siRNA was FAM- labeled and nucleus was stained with DAPI(blue). SMC: siRNA-MPG complex, SO: siRNA only, FAM: 6-Carboxy- Fluorescein DAPI: 4',6-diamidino-2-phenylindole.

The mean count of cells displaying fluorescent speckles, which gives an idea of the transfection efficiency of MPG, was 84% in Day 3 differentiating cells (Figure 19).

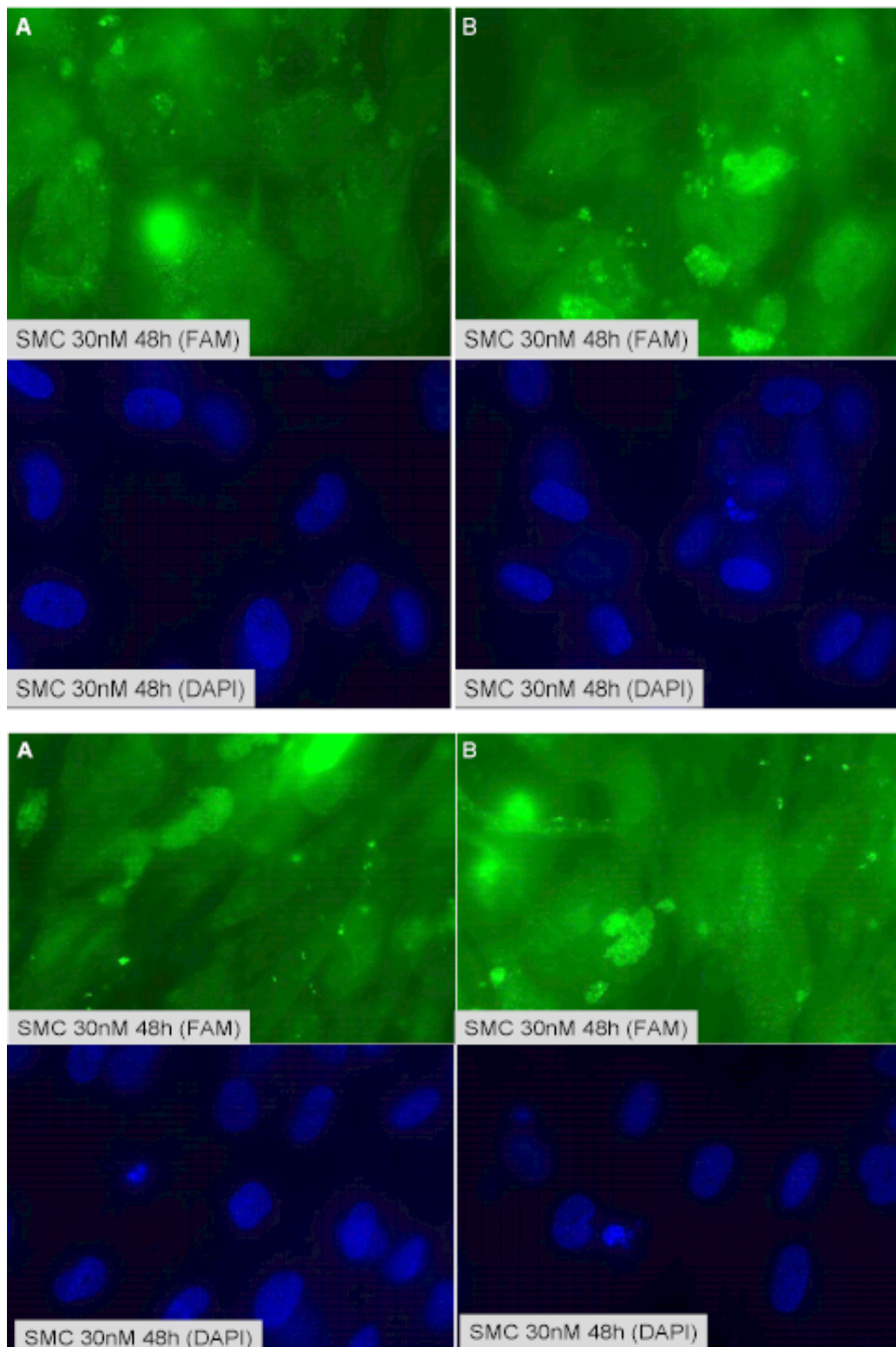


**Figure 19:** Fluorescence microscopy analysis 48h after transfection of differentiating hMADS cells at Day 3 of Induction. Cells were transfected for 4h with 30 nM siRNA-MPG complex (A and B). Stitched images used for cell counting to determine the percentage of transfection. Upper panel A (100%) and B (78.57%) Lower panel A (72.22%) and B (83.33%). The mean percentage fluorescent count was 83.53%.

### 3.3.8. siRNA-MPG complex is able to deliver double-stranded siRNA into differentiating hMADS cells (48h post-transfection analysis)

To assess the ability of MPG to deliver siRNA into Day 3 adipocyte differentiating cells, the cells were transfected for 4h with 30 nM SMC and control overlaid with SO for 4h. They were examined 48h post-transfection using Axioimager. Figure 20 (A) depicts the SMC in FAM channel (A) and the merged image of FAM, DAPI and Phase contrast (B). Punctuated fluorescence speckles were observed in the SMC within the cytoplasm.

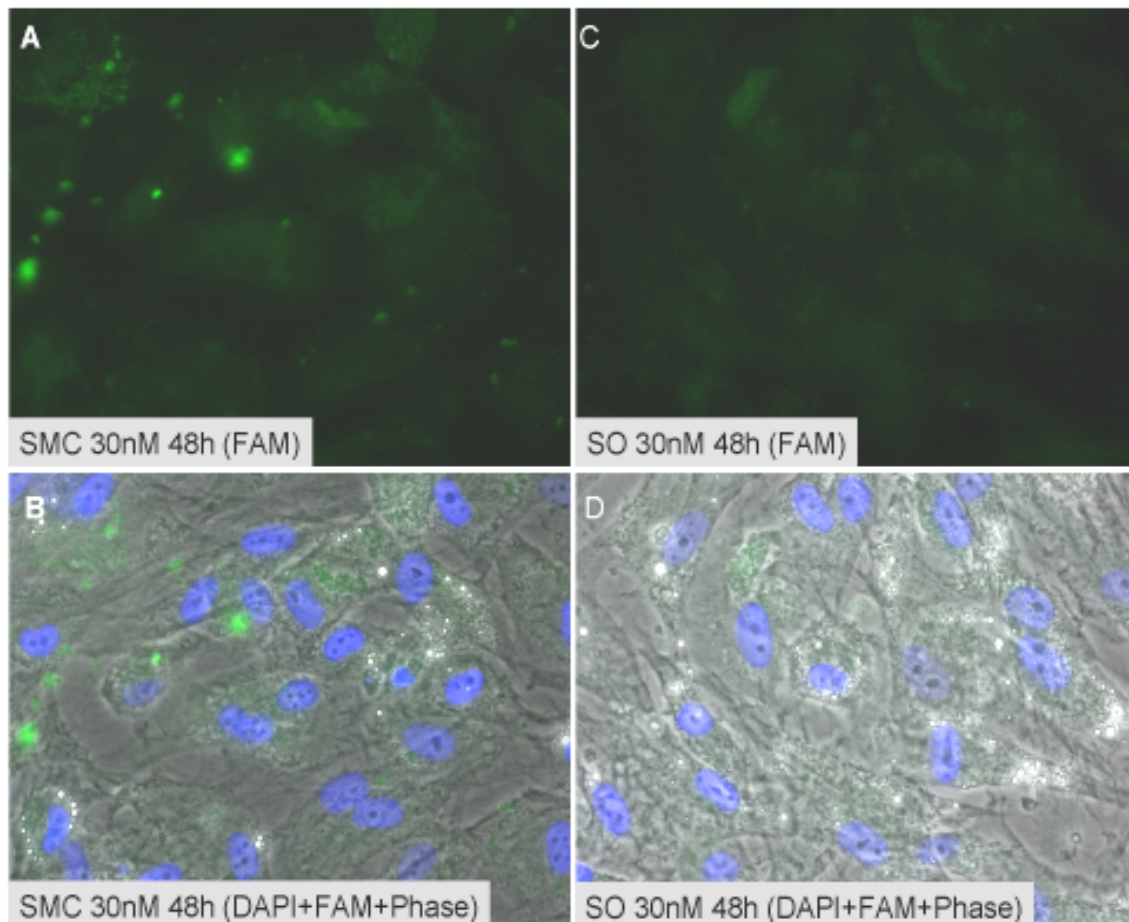


**Figure 20:** Fluorescence microscopy analysis 48h after transfection of differentiating hMADS cells at Day 3 of Induction. Cells were transfected for 4h with 30 nM siRNA-MPG complex (A and B). Punctuate fluorescent speckle were identified in cytoplasm of the cells (A and B). Control experiment (C and D): cells were overlaid for 4 h with free siRNA only. There was no fluorescent speckle present in the SO; however the cell background was visible. FAM channel (A and C) and nucleus was stained with DAPI (blue). SMC: siRNA-MPG complex, SO: siRNA only, FAM: 6'-carboxy fluorescein, DAPI: 4',6-diamidino-2-phenylindole.

In the control Figure 20 (C and D), no fluorescence was observed in the control SO. Maximum intensity projection MIP in Figure 21 demonstrated the presence of fluorescent speckles within the nucleus. In summary, there was both cytoplasmic and nuclear localization of the fluorescent speckles within the plane of the nucleus shown by the MIP image (Figure 21).

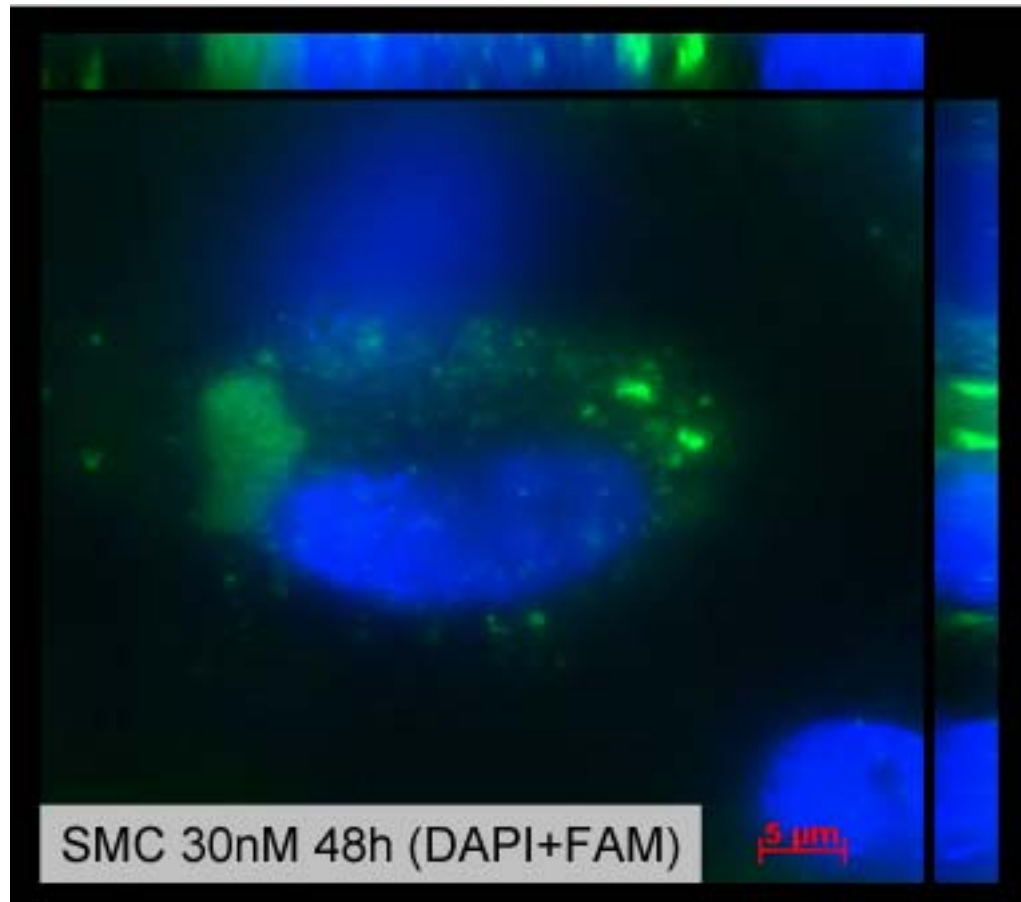


**Figure 21:** Fluorescence microscopy analysis 4h after transfection of differentiating hMADS cells at Day 3. Maximum intensity projection (MIP) punctuate fluorescent speckles of the labeled SMC were seen localized in the cytoplasm and in the nucleus. siRNA-MPG complex, SO: siRNA only, FAM: 6-Carboxy-Fluorescein, DAPI: 4',6-diamidino-2-phenylindole.

The results showed that MPG could deliver labeled siRNA into the cytoplasm and nucleus of Day 3 adipocyte differentiating cells.

### 3.3.9. Transfection of differentiating cells at Day 10

To investigate whether SMC was delivered into Day 10 adipocyte differentiating cells, the cells were transfected for 4h with 30 nM SMC and control overlaid with SO for 4h. They were examined 48h post-transfection using Axioimager. Figure 22 (A, B) depict the SMC in FAM channel (A) and the merged image of FAM, DAPI, and Phase contrast (B). Stronger fluorescence speckles were observed in the SMC within the cytoplasm that showed a more condensed pattern. The speckles were also detected within some fat droplets. Although some background fluorescence was observed in SO, there was clear difference between the control and the SMC transfected cells.

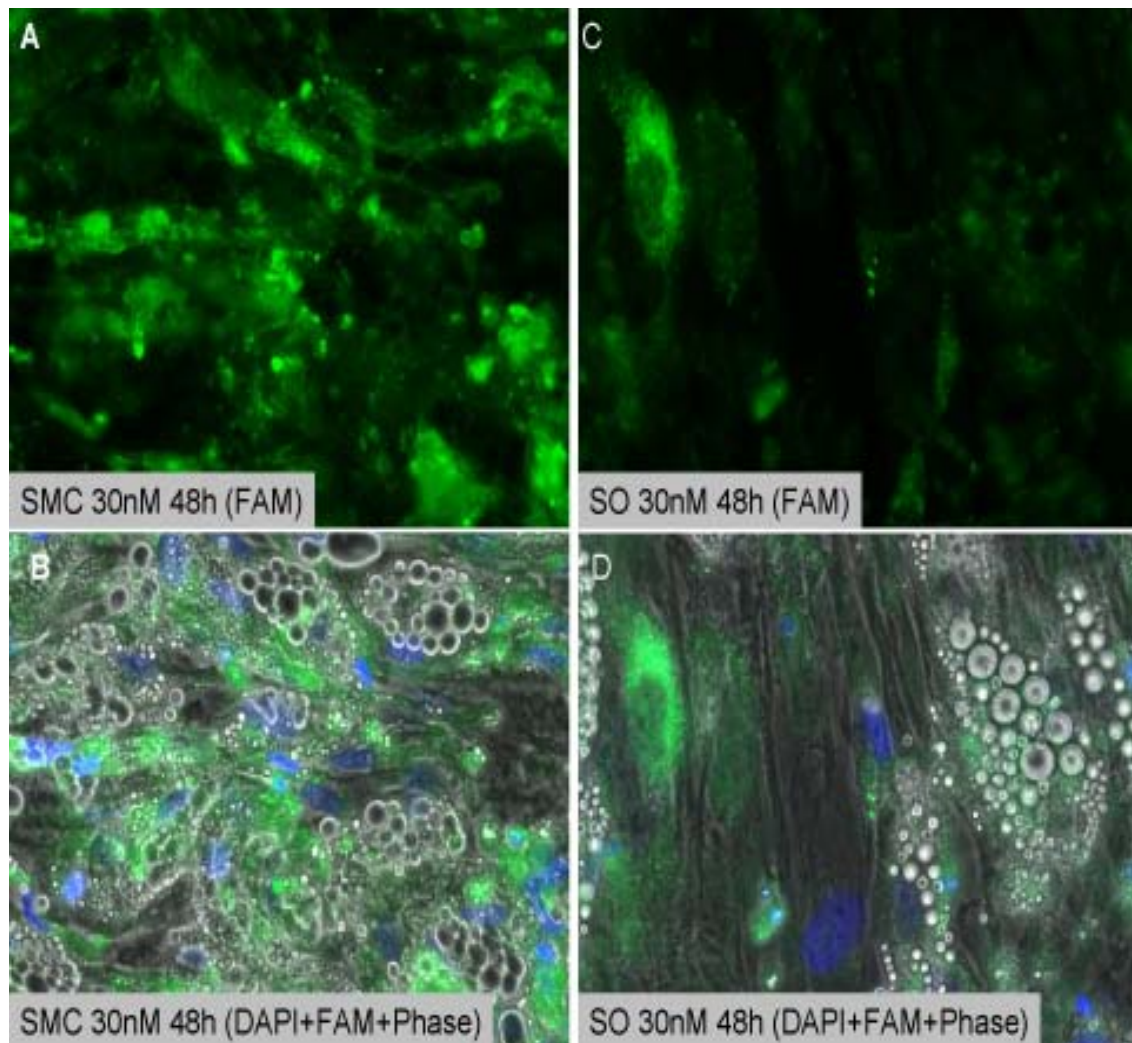


**Figure 22:** Fluorescence microscopy analysis 48h post-transfection of adipocyte differentiating hMADS cells at Day 10. Cells were transfected for 4h with 30 nM siRNA-MPG complex (SMC). A (FAM) B (DAPI, FAM, Phase contrast) stronger fluorescence speckles were observed in the SMC that showed more condensed pattern in FAM channel. Control experiment (C,D): cells were overlaid for 4h with free siRNA only. C: FAM. D: (merged image of DAPI, FAM, Phase contrast). The observed fluorescence was due to back-ground which were weaker than those of the SMC.

Nucleus was stained with DAPI (blue). SMC: siRNA-MPG complex, SO: siRNA only, FAM: 6-carboxy-Fluorescein, DAPI: 4',6-diamidino-2-phenylindole

Maximum intensity projection (MIP) equally demonstrated the presence of the fluorescent speckle within the nucleus which suggests nuclear localization of the siRNA construct. In summary, there was both cytoplasmic and nuclear localization of the fluorescent speckle within the plane of the nucleus shown by the MIP image (Figure 23).

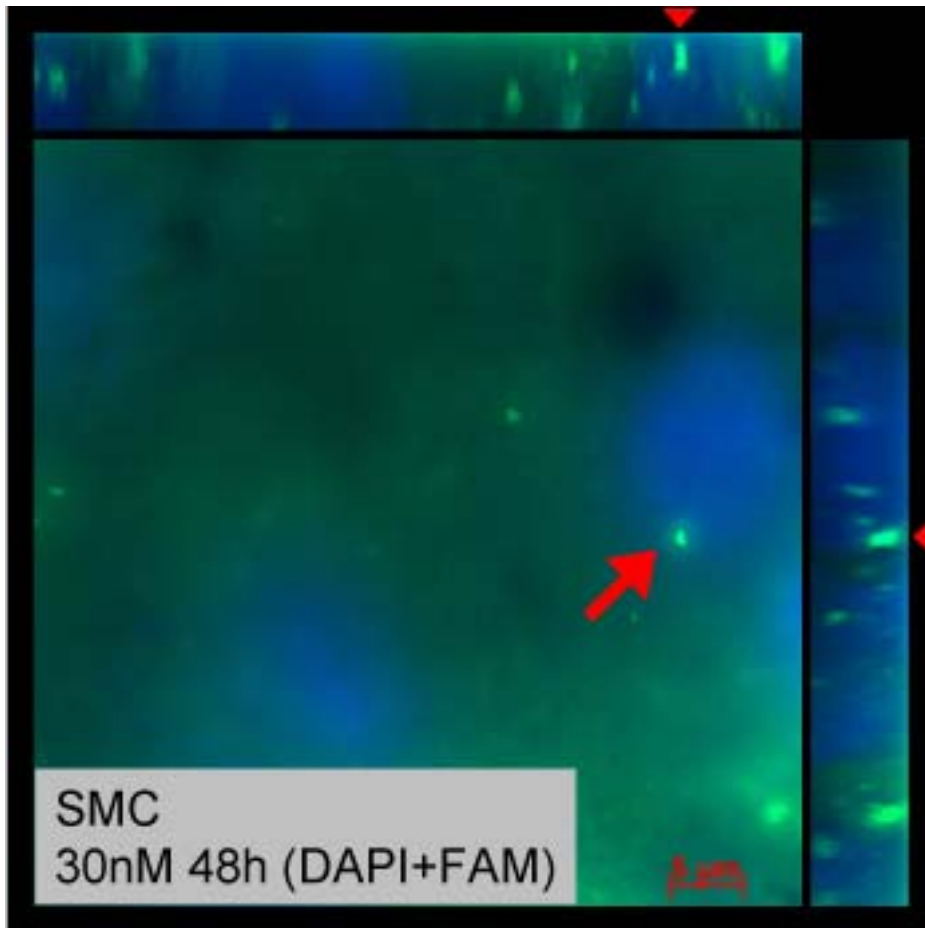


**Figure 23:** Fluorescence microscopy analysis 48h after transfection of adipocyte differentiated hMADS cells at Day 10. Maximum intensity projection MIP, of the fluorescent speckles were seen in the cytoplasm (red arrow) indicating that the punctuate speckles of SMC lies within the cytoplasm at the plane of the nucleus. siRNA was FAM-labeled and nucleus was stained with DAPI (blue). SMC: siRNA-MPG complex, SO: siRNA only, FAM: 6-Carboxy- Fluorescein DAPI: 4',6-diamidino-2-phenylindole.

The results showed that MPG could deliver labeled siRNA into the cytoplasm and nucleus of Day 10 adipocyte differentiating cells.

## 4. DISCUSSION

Divita and co-workers reported that MPG delivers active macromolecules permitting the control of the release of the cargo in the appropriate target subcellular compartment. Therefore, by tampering with the NLS sequence of MPG, delivery between the nucleus and the cytoplasm can be discriminated and MPG containing the NLS efficiently was reported to deliver promoter-directed siRNA into the nucleus to inhibit transcription. MPG has also been successfully applied for delivery of siRNA *in vivo* into mouse blastocytes (Crombez et al., 2007b) The results presented here are in agreement with the earlier report by Simeoni et al (2003) showing that MPG mediates cytoplasmic and nuclear delivery of siRNA in many cell types.

### 4.1. Viability

Effect of MPG on the viability of hMADS cells transfected with 15nM and 30nM of SMC and during proliferation and in adipocyte differentiation show that there was no observed cytotoxicity associated with the complex. There was no cell mortality or distortion of cell morphology due to the MPG complex. These results demonstrate that MPG while efficiently delivering siRNA into hMADS cells, it preserves the cell structural integrity. The complex had a mild effect on the cells. Most lipid based transfection agents according to Zaragosi lead to low cell viability or induce cell toxicity in the course of transfection. Unpublished report on hMADS also showed that electroporation of hMADS cell also led to high cell mortality. In view of these, MPG presents a mild transfection possibility in hMADS cells.

### 4.2. Differentiation

Data from this study also showed that differentiation of cells into adipocyte was not hindered by the transfection of hMADS cells with MPG-siRNA complex. There was no evidence to suggest that MPG adversely affected differentiation of hMADS cells to adipocytes as there were differentiated cells with oval shaped lipid droplets in both SMC treated and the cell only control (Figure 8 lower panel). The siRNA used in the study was a scrambled control not targeting any specific messenger RNA, so it was not meant to affect differentiation process.

### 4.3. siRNA delivery in proliferation and in adipocyte differentiation

This study was designed to evaluate the MPG mediated delivery of Double stranded siRNA into hMADS cells. hMADS cells have been shown to be difficult to transfect with plethora of conventional lipid based transfection system (Zaragosi et al., 2007a). Zaragosi and colleagues reported very low transfection efficiency coupled with high cell mortality in respect of transfection with lipid based reagents. But they reported high efficiency of delivery with Nucleofection for both stable and transient integration of transgenes into hMADS cells. The results of this study show that MPG successfully delivered double-stranded 5' 6-FAM labeled siRNA into hMADS cells in pre-confluent, confluent and adipocyte differentiated hMADS cells. Delivery efficiency as monitored by detection of fluorescence in the MPG transfected cells was significantly higher than in the control groups. The transfection efficiency of the delivered siRNA was above 90-95% in the confluent hMADS cells 24h post-transfection, the retention of fluorescence 48h and 72h were however weak and was between 50-60% efficiency. Using Olympus CKX41 microscope evidence of siRNA delivery was apparent as indicated by punctuate fluorescence speckles after 4h post-transfection this indicates that the internalization was rapid. Fluorescence was detectable up to 6 days post-transfection in confluent stage.

However, the exact localization of the observed fluorescence in this case could not be resolved, as such could not be said to be inside or outside the cell due to the limitation of the microscope used. Fluorescence in the pre-confluent stage was detected 24h and 48h post-transfection, at a concentration of 15 nM of SMC. In the confluent and differentiated stages detection was after 24h to 72h at a concentration of 30nM of SMC.

In the Day 10 adipocyte differentiated cells, stronger fluorescence speckles were detected in the SMC within the cytoplasm that showed a more condensed pattern. The speckles were also observed within some fat droplets. However, some background fluorescence was present in SO that could not be readily explained. This background fluorescence might be due to auto-fluorescence of the lipid droplets that were well developed in the Day 10. However, there was clear difference between the control and the SMC transfected cells. Maximum intensity projection MIP (Figure 22) equally demonstrated the presence of the fluorescent speckle within the nucleus which suggests nuclear localization of the siRNA construct. In summary, there was both cytoplasmic and nuclear localization of the fluorescent speckle within the plane of the nucleus shown by the MIP image. The results showed that MPG could deliver labeled siRNA into the cytoplasm and nucleus of Day 10 adipocyte differentiated cells. The MIP images showed the fluorescence speckles within the nucleus as well as within the cytoplasm at the plane of the nucleus, demonstrating internalization of double-stranded siRNA mediated by MPG.

#### 4.4. Pattern of delivery

The delivered siRNA was detected as brilliant punctuated fluorescent speckles in the green channel that was not homogeneously distributed in the cells. This observation was in line with the observation of (Veldhoen et al., 2006a) who worked on similar peptide but with a mutation at the nuclear localization sequence, called MPG $\alpha$ . The bright speckles are thought to mark points of entry of the labelled probes into the cells. But contrary to their observation MPG efficiently delivered siRNA into the cytoplasm as well as nucleus of hMADS cells. Gregory et al (2007) also observed punctuate and non-homogeneously distributed pattern of delivery of cargo with TAT peptide. It then follows that the punctuate spotted fluorescent speckle observed in the SMC transfected cells were indicative of successful internalization of siRNA in the cytoplasm, nuclear membrane and in the nucleus as observed in the results presented in this study. The pattern of internalization was contrary to most convectional transfection reagents which usually follow homogenous distribution pattern in most cell types. But MPG here showed dotted or punctuated fluorescent speckles within the cells transfected with SMC. The control group overlaid with free siRNA did not show these green fluorescent speckles. The same observation was true for the cell only (CO) control group which did not have the speckle. However, there was background green fluorescence in the control sometimes highlighting the cell inside, which was instructive in determining whether the fluorescence was inside or outside the cell.

The result of this work demonstrated that Nucleofection is not the only non-viral based vector that has the ability of efficiently transfecting hMADS cells as observed by Zaragosi and colleagues (Zaragosi et al., 2007c). The benefit of Nucleofection was the achievement of stable expression of a transgene in hMADS cells. However, the internalization of siRNA observed with MPG is transient as fluorescence intensity weakened with time but was detectable 6 days post-transfection.

In summary, this study could demonstrate that MPG efficiently internalized labeled double-stranded siRNA cargo into the difficult to transfect hMADS cells in proliferation, confluency, and adipocyte differentiating hMADS cells. That MPG mediated nuclear localization of siRNA constructs supports the observation of Divita and co-workers (Crombez et al., 2007b; Simeoni et al., 2005). More interesting is that transduction of non-

dividing cell has been the preserve of the lentiviral system which is limited by their high bio safety requirement and as such are kept out of routine use of many laboratory. However, lentiviral systems are used for stable integration into the genome of cells while CPPs can only be used for transient internalization. MPG did not lead to cell mortality as indicated by the normal cell morphology exhibited by the SMC transfected cells, which was comparable to the morphology of the siRNA only (SO) and cell only (CO) overlaid control groups. This observation makes MPG an interesting vector system for translocation of small peptides and nucleic acids into the cell combining robust efficiency of delivery with mildness to the cell structure integrity.

## 5. CONCLUSION

In conclusion, this study showed that MPG efficiently delivered double-stranded siRNA into the nucleus and cytoplasm of hMADS cells. The efficiency of delivery was between 90-95% in the pre -confluent and confluent stages 24h post-transfection, 84% in Day 3 differentiating cells 24h post-transfection. The efficiency of the delivery 48h and 72h post-transfection was between 50-60%. The cell viability was not adversely affected while differentiation of hMADS cells proceeded normally. These results show that MPG is a very effective and robust non-viral based transfection agent that efficiently translocates hMADS cells to transiently deliver siRNA. The integration was transient as it lasted for about 6 days.

### 5.1. Outlook

This study established that MPG could deliver double-stranded siRNA into hMADS cells, the nucleus and the cytoplasm. Further work will evaluate the delivery of single stranded siRNA which will set that stage for the use of microRNAs for knock-down of specific target genes for adipogenesis or other cell fate decisions. Future research focusing on improvement of targeting specificity of MPG should be encouraged.

## 6. ABBREVIATION

CO	Cell only
DAPI	4',6-diamidino-2-phenylindole
dsRNA	double-stranded RNA
FAM	6'-Carboxy-Fluorescein
hMADS	Cells- Human multipotent adipose- derived stem cells
MIP	maximum intensity projection
miRNA	microRNA
MSCs	Mensenchymal stem cells
RdRP	RNA-dependent RNA polymerase
RISC	RNA-induced silencing protein complex
RNAi	RNA interference
siRNA	short interfering RNA
SMC	siRNA-MPG complex
SO	siRNA only
stRNA	small temporal RNA
stRNA	small temporal RNA
UTR	untranslated region

## 7. APPENDIX

### 7.1. PROTOCOL FOR N-TER–NANOPARTICLE MEDIATED DELIVERY OF siRNA INTO (hMADS)

#### Materials

1. N-TER Peptide (Sigma, Cat # N0538)
2. N-TER Buffer (Sigma, Cat # N0413)
3. 5' 6-FAM labeled Control siRNA (Sigma)
4. Sonicating water bath, (Elma, Transsonic 420, 35 kHz)
5. RNase free water
6. Microcentrifuge (Eppendorf)
7. Microfuge tubes
8. Phosphate buffered saline (PBS)
9. Serum free medium
10. Complete medium (DMEM)

#### Procedure

##### Quick overview of procedure

##### 1. Prepare Adherent Cells

Plate cells before transfection- 24hrs (Variable)

##### 2. Prepare N-TER Nanoparticle siRNA Complex -30mins

- a. Prepare siRNA Master stock solution
- b. Dilution N-TER peptide in water
- c. Preparation of nanoparticle formation solution, (NFS) by combining siRNA working solution and N-TER peptide/Buffer
- d. Incubate complex at 37 °C for 30-40 mins.

##### 3. Transfect Cells/ Knockdown Target- 24-72 hr

- a. Add complex, incubate 3-5 min at RT
- b. Add serum-free media, incubate 2-4 hr at 37 °C, 5% CO<sub>2</sub>
- c. Add complete media, incubate 24-72 hr at 37 °C, 5% CO<sub>2</sub>

##### 4. Quantify mRNA and/or Protein Knockdown

#### 2. a Preparation of siRNA stock/working solution

To prepare 50uM siRNA stock solution

- Dissolve 10.5nmoles dry siRNA in 210uL of RNase-free water.
- Store target/control siRNAs as a concentrated master stocks (typically 20-50 uM)
- separated into small aliquots.
- Dilute siRNA master stocks to 5 uM working stocks in RNase- free water as follows:
- To make 1ml of 5uM siRNA working solutions, dilute 100uL of the 50 uM stock solution in 900uL of RNase-free water.
- To prepare siRNA and N-TER buffer dilution of 5uM working solution, see table table1.

#### Formation of the N-TER Peptide/siRNA Nanoparticle complex, NFC (as in Sigma manual)

1. Thaw the N-TER Peptide and 5 uM siRNA working stocks at room temperature for ~10 minutes. Briefly vortex each tube and pulse-spin in a microcentrifuge. Store the siRNA working stocks on ice until they are needed.

2. Incubate the thawed N-TER Peptide in a sonicating water bath at maximum output and continuous power for 3-5 minutes.

Note: Incubation of the N-TER Peptide in a sonicating water bath is optional. However, this step decreases possible aggregation of the peptide and can reduce the variability of transfection efficiency.

3. While the N-TER Peptide is in the sonicating water bath, dilute the 5  $\mu$ M siRNA working stocks with N-TER Buffer in a sterile tube (see Table 1).

Briefly vortex each tube and pulse-spin in a microcentrifuge.

Store the diluted siRNAs on ice until they are needed.

**Table 1. Dilution of 5  $\mu$ M siRNA working stocks in N-TER Buffer**

Reagent	Tube 1A Target siRNA	Tube 2A Neg. control siRNA	Tube 3A Cells only control
5 $\mu$ M target siRNA working stock ( $\mu$ L)	39	0	0
5 $\mu$ M negative control siRNA working stock ( $\mu$ L)	0	19.5	0
N-TER Buffer ( $\mu$ L)	111	55.5	75
FINAL VOLUME ( $\mu$ L)	150	75	75

**Table1b. (siRNA control)**

Reagent	Tube1A	Tube2A
5uM siRNA control(uL)	39	
N-TER Buffer (uL)	111	75
Final volume (uL)	150	75

## 2. b. Dilution of N-TER peptide in water

4. Dilute the N-TER Peptide into water in a sterile tube (Table 2). Briefly vortex each tube and pulse-spin in a microcentrifuge.

-Incubate the diluted N-TER Peptide in a sonicating water bath at maximum output and continuous power for 3-5 minutes.

**Table2. Dilution of N-TER peptide in water.**

Reagent	Tube 1B Target siRNA	Tube 2B Neg. control siRNA	Tube 3B Cells only control
N-TER Peptide ( $\mu$ L)	24	12	0
Water ( $\mu$ L)	126	63	75
FINAL VOLUME ( $\mu$ L)	150	75	75

**Table 2b. (siRNA control)**

Reagent	Tube1B	Tube2B
N-TER Peptide (uL)	24	0
Water (uL)	126	75
Final volume (uL)	150	75

5. Prepare the Nanoparticle Formation Solutions by combining the appropriate diluted siRNA solutions with diluted N-TER Peptide solutions by adding the contents of Tube 1A through 3A to Tube 1B through 3B, respectively (see Tables 1 and 2).

-Briefly vortex each tube and pulse-spin in a microcentrifuge.

6. Incubate the tubes containing the Nanoparticle Formation Solution (combined siRNA and N-TER Peptide solutions) at 37 °C for 30-45 minutes to allow the nanoparticles to form.

Note: The concentration of the siRNA in the Nanoparticle Formation Solution is 650 nM at this point.

## 2. c Dilution of the Nanoparticle Formation solutions with 0.5x N-TER Buffer .

### Preparation of 0.5x N-TER Buffer

1. Combine equal volumes of water and N-TER Buffer to make 3 mL of 0.5x N-TER buffer. (Add 1500uL of N-TER buffer to 1500uL of water to make 3mL of 0.5x Buffer)

- Use this mix for dilution of the Nanoparticle Formation Solution to the appropriate concentrations (as shown in table 3)
- Vortex to mix and pulse-spin in a microcentrifuge.

2. Table 3 shows a dilution series for assay of a range of target siRNA concentrations. Dilute the 650 nM Nanoparticle Formation Solution (NFS= with 0.5x N-TER Buffer as indicated.

- Briefly vortex each tube and pulse-spin in a microcentrifuge.

**Table 3: Dilution of nanoparticles in 0.5x N-TER Buffer**

Reagent	[siRNA] <sub>final</sub> (nM)				
	30	20	10	5	2.5
Nanoparticle Formation Solution (μL)	111	74	37	18	9
0.5x N-TER Buffer (μL)	339	376	413	432	441

3. Dilute the negative control Nanoparticle Formation Solution as indicated in the first column ([siRNA]<sub>final</sub> of 30 nM) of Table 3.

4. Dilute 14 uL of the target siRNA into 436 uL of 0.5x N-TER Buffer to use as the “siRNA only control.” Briefly vortex each tube and pulse-spin in a microcentrifuge.

5. Dilute the 150 uL of Cells only control (Tube 3 in Tables 1 and 2) with 300 uL of 0.5x N-TER Buffer.

Note: Each of the above target siRNA and control dilutions will provide enough material for up to 15 replicates of 96 well plate, 1 well of 6well plate.

## 3. Transfection of adherent cells

1. Carefully remove the medium from each 6 well plate, then wash each well with 1.5mL of PBS, pH 7.4. Be careful to avoid disturbing the cell layer at the bottom of the wells.

2. Transfer 300uL of the diluted Nanoparticle Formation Solution ([siRNA] final of 30 nM) to each well of a 6 well culture plate. Repeat this step with the controls also. Gently rock the plate to evenly distribute the liquid over the surface of the cells. Incubate the plate at room temperature for 3-5 minutes.
3. Carefully add 300uL of serum and antibiotics-free medium to each well.
4. Incubate the plates under standard cell culture conditions, typically 37 °C and 5% CO<sub>2</sub>, for 2-4 hours.
6. Add 1000uL of complete medium to each well.
7. Incubate the plates under standard cell culture conditions, typically 37 °C and 5% CO<sub>2</sub>, for 24-48 hours.
8. Remove the complex-media mixture and wash with 1.5ml PBS.
9. Repeat the washing step for 2x.
10. Replace with 2ml complete media.
11. Fluorescence microscopy.

## 8. LIST OF FIGURES

- Figure 1: Gene silencing by endogenous and exogenous hairpin-like transcripts, Page 8  
Figure 2: miRNA biogenesis and post-transcriptional gene regulation by miRNAs, Page 10  
Figure 3: Mechanism of cellular uptake of MPG–siRNA complexes, Page 16  
Figure 4: Schematic model depicting adult stem cell differentiation, Page 17  
Figure 5: Models of mesenchymal stem cell differentiation, Page 18  
Figure 6: Zeiss Axioimager, Page 26  
Figure 7: Differentiation of hMADS, Page 28  
Figure 8: Cell viability, Page 29  
Figure 9: Transfection of hMADS cells 48h post-transfection, Page 32  
Figure 10: Transfection of hMADS cells 24h post-transfection Page 33  
Figure 11: Transfection of hMADS cells 24h post-transfection (MIP), Page 34  
Figure 12: Transfection of confluent hMADS cells 24h post-transfection, Page 35  
Figure 13: Transfection of confluent hMADS cells 24h post-transfection, Page 36  
Figure 14: Transfection of confluent hMADS cells 24h post-transfection (MIP), Page 37  
Figure 15: Transfection of confluent hMADS cells 48h post-transfection, Page 32  
Figure 16: Transfection of confluent hMADS cells 48h post-transfection, Page 39  
Figure 17: Transfection of D10 hMADS cells 72h post-transfection, Page 40  
Figure 18: Transfection of D10 hMADS cells 48h post-transfection (Cell count), Page 42  
Figure 19: Transfection of D10 hMADS cells 48h post-transfection (MIP) Page 41  
Figure 20: Transfection of D3 hMADS cells 48h post-transfection, Page 43  
Figure 21: Transfection of D3 hMADS cells 72h post-transfection (MIP) Page 44  
Figure 22: Transfection of D10 hMADS cells 48h post-transfection, Page 45  
Figure 23: Transfection of D10 hMADS cells 48h post-transfection(MIP), Page 46

## 9. LIST OF TABLES

- Table 1: Constituents of Proliferation medium  
Table 2: Constituents of Differentiation Medium.  
Table 3: Transfection Reagents  
Table 4: Equipment  
Table 5: Dilution of 5 uM siRNA working solution in MPG Buffer.  
Table 6: Dilution of MPG in water  
Table 7: Dilution of SMC in 0.5x MPG Buffer

## 10. REFERENCE

- Agami,R., 2002b. RNAi and related mechanisms and their potential use for therapy. *Curr Opin Chem Biol* 6, 829-834.
- Agami,R., 2002a. RNAi and related mechanisms and their potential use for therapy. *Curr Opin Chem Biol* 6, 829-834.
- Aigner,A., 2006. Delivery Systems for the Direct Application of siRNAs to Induce RNA Interference (RNAi) In Vivo. *J. Biomed. Biotechnol.* 2006, 71659.
- Ailhaud,G., 2000. Adipose tissue as an endocrine organ. *Int. J. Obes. Relat Metab Disord.* 24 Suppl 2, S1-S3.
- Arenz,C., Schepers,U., 2003. RNA interference: from an ancient mechanism to a state of the art therapeutic application? *Naturwissenschaften* 90, 345-359.
- Astriab-Fisher,A., Sergueev,D., Fisher,M., Shaw,B.R., Juliano,R.L., 2002. Conjugates of antisense oligonucleotides with the Tat and antennapedia cell-penetrating peptides: effects on cellular uptake, binding to target sequences, and biologic actions. *Pharm Res* 19, 744-754.
- Baksh,D., Davies,J.E., Zandstra,P.W., 2003. Adult human bone marrow-derived mesenchymal progenitor cells are capable of adhesion-independent survival and expansion. *Exp Hematol* 31, 723-732.
- Baksh,D., Song,L., Tuan,R.S., 2004. Adult mesenchymal stem cells: characterization, differentiation, and application in cell and gene therapy. *J Cell Mol Med* 8, 301-316.
- Bartel,D.P., 2004. MicroRNAs: genomics, biogenesis, mechanism, and function. *Cell* 116, 281-297.
- Birmingham,A., Anderson,E.M., Reynolds,A., Ilsley-Tyree,D., Leake,D., Fedorov,Y., Baskerville,S., Maksimova,E., Robinson,K., Karpilow,J., Marshall,W.S., Khvorova,A., 2006. 3' UTR seed matches, but not overall identity, are associated with RNAi off-targets. *Nat Methods* 3, 199-204.
- Christiaens,B., Symoens,S., Verheyden,S., Engelborghs,Y., Joliot,A., Prochiantz,A., Vandekerckhove,J., Rosseneu,M., Vanloo,B., 2002. Tryptophan fluorescence study of the interaction of penetratin peptides with model membranes. *Eur J Biochem* 269, 2918-2926.
- Crombez,L., Charnet,A., Morris,M.C., Aldrian-Herrada,G., Heitz,F., Divita,G., 2007a. A non-covalent peptide-based strategy for siRNA delivery. *Biochem. Soc. Trans.* 35, 44-46.
- Crombez,L., Charnet,A., Morris,M.C., Aldrian-Herrada,G., Heitz,F., Divita,G., 2007b. A non-covalent peptide-based strategy for siRNA delivery. *Biochem Soc Trans* 35, 44-46.
- Dani,C., Doglio,A., Amri,E.Z., Bardou,S., Fort,P., Bertrand,B., Grimaldi,P., Ailhaud,G., 1989a. Cloning and regulation of a mRNA specifically expressed in the preadipose state. *J. Biol. Chem.* 264, 10119-10125.

- Dani,C., Doglio,A., Amri,E.Z., Bardon,S., Fort,P., Bertrand,B., Grimaldi,P., Ailhaud,G., 1989b. Cloning and regulation of a mRNA specifically expressed in the preadipose state. *J. Biol. Chem.* 264, 10119-10125.
- Derossi,D., Calvet,S., Trembleau,A., Brunissen,A., Chassaing,G., Prochiantz,A., 1996b. Cell internalization of the third helix of the Antennapedia homeodomain is receptor-independent. *J. Biol. Chem.* 271, 18188-18193.
- Derossi,D., Calvet,S., Trembleau,A., Brunissen,A., Chassaing,G., Prochiantz,A., 1996a. Cell internalization of the third helix of the Antennapedia homeodomain is receptor-independent. *J. Biol. Chem.* 271, 18188-18193.
- Derossi,D., Chassaing,G., Prochiantz,A., 1998. Trojan peptides: the penetratin system for intracellular delivery. *Trends Cell Biol* 8, 84-87.
- Derossi,D., Joliot,A.H., Chassaing,G., Prochiantz,A., 1994b. The third helix of the Antennapedia homeodomain translocates through biological membranes. *J. Biol. Chem.* 269, 10444-10450.
- Derossi,D., Joliot,A.H., Chassaing,G., Prochiantz,A., 1994a. The third helix of the Antennapedia homeodomain translocates through biological membranes. *J. Biol. Chem.* 269, 10444-10450.
- Derossi,D., Joliot,A.H., Chassaing,G., Prochiantz,A., 1994c. The third helix of the Antennapedia homeodomain translocates through biological membranes. *J. Biol. Chem.* 269, 10444-10450.
- Deshayes,S., Gerbal-Chaloin,S., Morris,M.C., Aldrian-Herrada,G., Charnet,P., Divita,G., Heitz,F., 2004. On the mechanism of non-endosomal peptide-mediated cellular delivery of nucleic acids. *Biochim Biophys Acta* 1667, 141-147.
- Deshayes,S., Morris,M.C., Divita,G., Heitz,F., 2005. Cell-penetrating peptides: tools for intracellular delivery of therapeutics. *Cell Mol Life Sci* 62, 1839-1849.
- Dietz,G.P., Bahr,M., 2004. Delivery of bioactive molecules into the cell: the Trojan horse approach. *Mol Cell Neurosci* 27, 85-131.
- Dykxhoorn,D.M., Palliser,D., Lieberman,J., 2006. The silent treatment: siRNAs as small molecule drugs. *Gene Ther* 13, 541-552.
- El Andaloussi,S., Holm,T., Langel,U., 2005a. Cell-penetrating peptides: Mechanisms and applications. *Current Pharmaceutical Design* 11, 3597-3611.
- El Andaloussi,S., Holm,T., Langel,U., 2005c. Cell-penetrating peptides: mechanisms and applications. *Curr Pharm Des* 11, 3597-3611.
- El Andaloussi,S., Holm,T., Langel,U., 2005b. Cell-penetrating peptides: mechanisms and applications. *Curr Pharm Des* 11, 3597-3611.
- Elbashir,S.M., Harborth,J., Weber,K., Tuschl,T., 2002. Analysis of gene function in somatic mammalian cells using small interferingRNAs. *Methods* 26, 199-213.
- Elbashir,S.M., Martinez,J., Patkaniowska,A., Lendeckel,W., Tuschl,T., 2001. Functional anatomy of siRNAs for mediating efficient RNAi in *Drosophila melanogaster* embryo lysate. *EMBO J* 20, 6877-6888.

- Esau,C., Kang,X., Peralta,E., Hanson,E., Marcusson,E.G., Ravichandran,L.V., Sun,Y., Koo,S., Perera,R.J., Jain,R., Dean,N.M., Freier,S.M., Bennett,C.F., Lollo,B., Griffey,R., 2004. MicroRNA-143 regulates adipocyte differentiation. *J Biol Chem* 279, 52361-52365.
- Filipowicz,W., Jaskiewicz,L., Kolb,F.A., Pillai,R.S., 2005. Post-transcriptional gene silencing by siRNAs and miRNAs. *Curr Opin Struct Biol* 15, 331-341.
- Fire,A., 1999. RNA-triggered gene silencing. *Trends Genet* 15, 358-363.
- Fire,A., Xu,S., Montgomery,M.K., Kostas,S.A., Driver,S.E., Mello,C.C., 1998. Potent and specific genetic interference by double-stranded RNA in *Caenorhabditis elegans*. *Nature* 391, 806-811.
- Frankel,A.D., Pabo,C.O., 1988. Cellular uptake of the tat protein from human immunodeficiency virus. *Cell* 55, 1189-1193.
- Gary,D.J., Puri,N., Won,Y.Y., 2007a. Polymer-based siRNA delivery: perspectives on the fundamental and phenomenological distinctions from polymer-based DNA delivery. *J. Control Release* 121, 64-73.
- Gary,D.J., Puri,N., Won,Y.Y., 2007b. Polymer-based siRNA delivery: perspectives on the fundamental and phenomenological distinctions from polymer-based DNA delivery. *J. Control Release* 121, 64-73.
- Gary,D.J., Puri,N., Won,Y.Y., 2007c. Polymer-based siRNA delivery: perspectives on the fundamental and phenomenological distinctions from polymer-based DNA delivery. *J. Control Release* 121, 64-73.
- Gregoire,F.M., Smas,C.M., Sul,H.S., 1998. Understanding adipocyte differentiation. *Physiol Rev.* 78, 783-809.
- Gregory,R.I., Chendrimada,T.P., Cooch,N., Shiekhattar,R., 2005. Human RISC Couples MicroRNA Biogenesis and Posttranscriptional Gene Silencing. *Cell*.
- Horwitz,E.M., Gordon,P.L., Koo,W.K., Marx,J.C., Neel,M.D., McNall,R.Y., Muul,L., Hofmann,T., 2002. Isolated allogeneic bone marrow-derived mesenchymal cells engraft and stimulate growth in children with osteogenesis imperfecta: Implications for cell therapy of bone. *Proc. Natl. Acad. Sci. U. S A* 99, 8932-8937.
- Huttenhofer,A., Schattner,P., Polacek,N., 2005. Non-coding RNAs: hope or hype? *Trends Genet* 21, 289-297.
- Jarver,P., Langel,U., 2004. The use of cell-penetrating peptides as a tool for gene regulation. *Drug Discov Today* 9, 395-402.
- Jarver,P., Langel,U., 2006. Cell-penetrating peptides--a brief introduction. *Biochim Biophys Acta* 1758, 260-263.
- Jiang,Y., Jahagirdar,B.N., Reinhardt,R.L., Schwartz,R.E., Keene,C.D., Ortiz-Gonzalez,X.R., Reyes,M., Lenvik,T., Lund,T., Blackstad,M., Du,J., Aldrich,S., Lisberg,A., Low,W.C., Largaespada,D.A., Verfaillie,C.M., 2002. Pluripotency of mesenchymal stem cells derived from adult marrow. *Nature* 418, 41-49.

- Kajimoto,K., Naraba,H., Iwai,N., 2006d. MicroRNA and 3T3-L1 pre-adipocyte differentiation. *RNA* 12, 1626-1632.
- Kajimoto,K., Naraba,H., Iwai,N., 2006b. MicroRNA and 3T3-L1 pre-adipocyte differentiation. *RNA* 12, 1626-1632.
- Kajimoto,K., Naraba,H., Iwai,N., 2006c. MicroRNA and 3T3-L1 pre-adipocyte differentiation. *RNA* 12, 1626-1632.
- Kajimoto,K., Naraba,H., Iwai,N., 2006a. MicroRNA and 3T3-L1 pre-adipocyte differentiation. *RNA* 12, 1626-1632.
- Koc,O.N., Gerson,S.L., Cooper,B.W., Dyhouse,S.M., Haynesworth,S.E., Caplan,A.I., Lazarus,H.M., 2000. Rapid hematopoietic recovery after coinfusion of autologous-blood stem cells and culture-expanded marrow mesenchymal stem cells in advanced breast cancer patients receiving high-dose chemotherapy. *J. Clin. Oncol.* 18, 307-316.
- Le,R., I, Joliot,A.H., Bloch-Gallego,E., Prochiantz,A., Volovitch,M., 1993. Neurotrophic activity of the Antennapedia homeodomain depends on its specific DNA-binding properties. *Proc. Natl. Acad. Sci. U. S A* 90, 9120-9124.
- Lim,L.P., Lau,N.C., Garrett-Engle,P., Grimson,A., Schelter,J.M., Castle,J., Bartel,D.P., Linsley,P.S., Johnson,J.M., 2005. Microarray analysis shows that some microRNAs downregulate large numbers of target mRNAs. *Nature* 433, 769-773.
- Lindgren,M., Hallbrink,M., Prochiantz,A., Langel,U., 2000. Cell-penetrating peptides. *Trends Pharmacol Sci* 21, 99-103.
- Liu,J., Valencia-Sanchez,M.A., Hannon,G.J., Parker,R., 2005. MicroRNA-dependent localization of targeted mRNAs to mammalian P-bodies. *Nat Cell Biol* 7, 719-723.
- Lund,E., Guttinger,S., Calado,A., Dahlberg,J.E., Kutay,U., 2004. Nuclear export of microRNA precursors. *Science* 303, 95-98.
- Martinez,J., Tuschl,T., 2004. RISC is a 5' phosphomonoester-producing RNA endonuclease. *Genes Dev.* 18, 975-980.
- Massiera,F., Saint-Marc,P., Seydoux,J., Murata,T., Kobayashi,T., Narumiya,S., Guesnet,P., Amri,E.Z., Negrel,R., Ailhaud,G., 2003. Arachidonic acid and prostacyclin signaling promote adipose tissue development: a human health concern? *J. Lipid Res.* 44, 271-279.
- Morris,K.V., Rossi,J.J., 2006a. Lentiviral-mediated delivery of siRNAs for antiviral therapy. *Gene Ther.* 13, 553-558.
- Morris,K.V., Rossi,J.J., 2006b. Lentiviral-mediated delivery of siRNAs for antiviral therapy. *Gene Ther.* 13, 553-558.
- Muratovska,A., Eccles,M.R., 2004. Conjugate for efficient delivery of short interfering RNA (siRNA) into mammalian cells. *FEBS Lett* 558, 63-68.
- Petite,H., Viateau,V., Bensaid,W., Meunier,A., de Pollak,C., Bourguignon,M., Oudina,K., Sedel,L., Guillemain,G., 2000. Tissue-engineered bone regeneration. *Nat. Biotechnol.* 18, 959-963.

- Pooga, M., Soomets, U., Hallbrink, M., Valkna, A., Saar, K., Rezaei, K., Kahl, U., Hao, J.X., Xu, X.J., Wiesenfeld-Hallin, Z., Hokfelt, T., Bartfai, T., Langel, U., 1998. Cell penetrating PNA constructs regulate galanin receptor levels and modify pain transmission in vivo. *Nat. Biotechnol.* 16, 857-861.
- Prochiantz, A., 1996. Getting hydrophilic compounds into cells: lessons from homeopeptides. *Curr. Opin. Neurobiol.* 6, 629-634.
- Ren, G., Li, T., Lan, J.Q., Wilz, A., Simon, R.P., Boison, D., 2007. Lentiviral RNAi-induced downregulation of adenosine kinase in human mesenchymal stem cell grafts: A novel perspective for seizure control. *Exp. Neurol.*
- Richard, J.P., Melikov, K., Vives, E., Ramos, C., Verbeure, B., Gait, M.J., Chernomordik, L.V., Lebleu, B., 2003. Cell-penetrating peptides: A reevaluation of the mechanism of cellular uptake. *J Biol Chem* 278, 585-590.
- Rodriguez, A.M., Elabd, C., Delteil, F., Astier, J., Vernochet, C., Saint-Marc, P., Guesnet, J., Guezennec, A., Amri, E.Z., Dani, C., Ailhaud, G., 2004b. Adipocyte differentiation of multipotent cells established from human adipose tissue. *Biochem Biophys Res Commun* 315, 255-263.
- Rodriguez, A.M., Elabd, C., Delteil, F., Astier, J., Vernochet, C., Saint-Marc, P., Guesnet, J., Guezennec, A., Amri, E.Z., Dani, C., Ailhaud, G., 2004c. Adipocyte differentiation of multipotent cells established from human adipose tissue. *Biochem Biophys Res Commun* 315, 255-263.
- Rodriguez, A.M., Elabd, C., Delteil, F., Astier, J., Vernochet, C., Saint-Marc, P., Guesnet, J., Guezennec, A., Amri, E.Z., Dani, C., Ailhaud, G., 2004a. Adipocyte differentiation of multipotent cells established from human adipose tissue. *Biochem. Biophys. Res. Commun.* 315, 255-263.
- Rodriguez, A.M., Pisani, D., Dechesne, C.A., Turc-Carel, C., Kurzenne, J.Y., Wdziekonski, B., Villageois, A., Bagnis, C., Breitmayer, J.P., Groux, H., Ailhaud, G., Dani, C., 2005a. Transplantation of a multipotent cell population from human adipose tissue induces dystrophin expression in the immunocompetent mdx mouse. *J Exp Med* 201, 1397-1405.
- Rodriguez, A.M., Pisani, D., Dechesne, C.A., Turc-Carel, C., Kurzenne, J.Y., Wdziekonski, B., Villageois, A., Bagnis, C., Breitmayer, J.P., Groux, H., Ailhaud, G., Dani, C., 2005b. Transplantation of a multipotent cell population from human adipose tissue induces dystrophin expression in the immunocompetent mdx mouse. *J Exp Med* 201, 1397-1405.
- Rosen, E.D., Spiegelman, B.M., 2000. Molecular regulation of adipogenesis. *Annu. Rev. Cell Dev. Biol.* 16, 145-171.
- Sheldon, K., Liu, D., Ferguson, J., Garipey, J., 1995. Lolligomers: design of de novo peptide-based intracellular vehicles. *Proc. Natl. Acad. Sci. U. S A* 92, 2056-2060.
- Simeoni, F., Morris, M.C., Heitz, F., Divita, G., 2003. Insight into the mechanism of the peptide-based gene delivery system MPG: implications for delivery of siRNA into mammalian cells. *Nucleic Acids Res* 31, 2717-2724.
- Simeoni, F., Morris, M.C., Heitz, F., Divita, G., 2005. Peptide-based strategy for siRNA delivery into mammalian cells. *Methods Mol. Biol.* 309, 251-260.

- Smas,C.M., Chen,L., Sul,H.S., 1997. Cleavage of membrane-associated pref-1 generates a soluble inhibitor of adipocyte differentiation. *Mol. Cell Biol.* 17, 977-988.
- Smas,C.M., Sul,H.S., 1993a. Pref-1, a protein containing EGF-like repeats, inhibits adipocyte differentiation. *Cell* 73, 725-734.
- Smas,C.M., Sul,H.S., 1993b. Pref-1, a protein containing EGF-like repeats, inhibits adipocyte differentiation. *Cell* 73, 725-734.
- Theodore,L., Derossi,D., Chassaing,G., Llibat,B., Kubes,M., Jordan,P., Chneiweiss,H., Godement,P., Prochiantz,A., 1995. Intraneuronal delivery of protein kinase C pseudosubstrate leads to growth cone collapse. *J. Neurosci.* 15, 7158-7167.
- Troy,C.M., Derossi,D., Prochiantz,A., Greene,L.A., Shelanski,M.L., 1996. Downregulation of Cu/Zn superoxide dismutase leads to cell death via the nitric oxide-peroxynitrite pathway. *J. Neurosci.* 16, 253-261.
- Tuschl,T., Zamore,P.D., Lehmann,R., Bartel,D.P., Sharp,P.A., 1999. Targeted mRNA degradation by double-stranded RNA in vitro. *Genes Dev* 13, 3191-3197.
- Veldhoen,S., Laufer,S.D., Trampe,A., Restle,T., 2006a. Cellular delivery of small interfering RNA by a non-covalently attached cell-penetrating peptide: quantitative analysis of uptake and biological effect. *Nucleic Acids Res.*
- Veldhoen,S., Laufer,S.D., Trampe,A., Restle,T., 2006b. Cellular delivery of small interfering RNA by a non-covalently attached cell-penetrating peptide: quantitative analysis of uptake and biological effect. *Nucleic Acids Res.*
- Weiner,F.R., Shah,A., Smith,P.J., Rubin,C.S., Zern,M.A., 1989. Regulation of collagen gene expression in 3T3-L1 cells. Effects of adipocyte differentiation and tumor necrosis factor alpha. *Biochemistry* 28, 4094-4099.
- Xu,P., Vernooy,S.Y., Guo,M., Hay,B.A., 2003. The Drosophila microRNA Mir-14 suppresses cell death and is required for normal fat metabolism. *Curr Biol* 13, 790-795.
- Yekta,S., Shih,I.H., Bartel,D.P., 2004. MicroRNA-directed cleavage of HOXB8 mRNA. *Science* 304, 594-596.
- Zaragosi,L.E., Ailhaud,G., Dani,C., 2006. Autocrine FGF2 signaling is critical for self-renewal of Human Multipotent Adipose-Derived Stem Cells. *Stem Cells* [Epub ahead of print].
- Zaragosi,L.E., Billon,N., Ailhaud,G., Dani,C., 2007c. Nucleofection is a valuable transfection method for transient and stable transgene expression in adipose tissue-derived stem cells. *Stem Cells* 25, 790-797.
- Zaragosi,L.E., Billon,N., Ailhaud,G., Dani,C., 2007a. Nucleofection is a valuable transfection method for transient and stable transgene expression in adipose tissue-derived stem cells. *Stem Cells* 25, 790-797.
- Zaragosi,L.E., Billon,N., Ailhaud,G., Dani,C., 2007b. Nucleofection is a valuable transfection method for transient and stable transgene expression in adipose tissue-derived stem cells. *Stem Cells* 25, 790-797.

- Zuk,P.A., Zhu,M., Ashjian,P., De Ugarte,D.A., Huang,J.I., Mizuno,H., Alfonso,Z.C., Fraser,J.K., Benhaim,P., Hedrick,M.H., 2002. Human adipose tissue is a source of multipotent stem cells. *Mol. Biol. Cell* 13, 4279-4295.
- Zuk,P.A., Zhu,M., Mizuno,H., Huang,J., Futrell,J.W., Katz,A.J., Benhaim,P., Lorenz,H.P., Hedrick,M.H., 2001b. Multilineage cells from human adipose tissue: implications for cell-based therapies. *Tissue Eng* 7, 211-228.
- Zuk,P.A., Zhu,M., Mizuno,H., Huang,J., Futrell,J.W., Katz,A.J., Benhaim,P., Lorenz,H.P., Hedrick,M.H., 2001a. Multilineage cells from human adipose tissue: implications for cell-based therapies. *Tissue Eng* 7, 211-228.